Investigation of Pramipexole as Potential Therapeutic Agent for Age-related Macular Degeneration

Keiichi Shibagaki

Nara Institute of Science and Technology

Graduate School of Biological Sciences

Laboratory of Molecular and Cell Genetics

Prof. Kenji Kohno

Date of submission: Jan. 9, 2015

Lab name （Supervisor）	Laboratory of Molecular and Cell Genetics (Prof. Kenji Kohno)		
Name	Keiichi Shibagaki	Date of submission	Dec.11, 2014
Title	Investigation of Pramipexole as Potential Therapeutic Agent for Age-related Macular Degeneration		

ABSTRACT

Age-related macular degeneration (AMD) is the most common cause of irreversible visual impairment of older adults in the developed world. Although the prevalence of AMD is increasing with the aging of the population, its etiology remains largely unclear. There are two major subtypes of AMD: the atrophic form, also called the dry type, and the neovascular form, also called the wet type. The former is characterized by geographic atrophy (GA) due to the death of the retinal pigment epithelium (RPE) and photoreceptor cells, and the latter develops due to choroidal neovascularization (CNV). Although wet AMD can be treated by anti-vascular endothelial growth factor (VEGF) agents, there is no approved therapeutic treatment available for dry AMD. Moreover, novel wet AMD treatment is also eagerly anticipated because anti-VEGF drugs have shown a broad range of effective response on wet AMD.

The purpose of this study was to investigate the potential of pramipexole, a potent dopamine receptor D2/D3 agonist, as a new treatment for AMD. To this end, I investigated its effect on light-induced retinal damage in mice, which is a model of dry AMD, and laser-induced CNV in rats, which is a model of wet AMD.

Pramipexole was orally administered 1 h before light exposure (5000 lux, 2 h). To evaluate the effect of ocular instillation of pramipexole, pramipexole solution was also applied to the cornea of mice 5 times a day for 2 days from the day before the light exposure. For combined administration, yohimbine, an alpha-2 adrenoceptor antagonist, was intraperitoneally injected 0.5 h prior to oral pramipexole treatment.

Electrophysiological and morphologic studies were performed to evaluate the effects of the test articles on light-induced retinal damage in mice 24 h after the light exposure. Oral administration and ocular instillation of pramipexole significantly prevented the reduction of the a- and b-wave electroretinogram (ERG) amplitudes caused by light exposure. In parallel, damage of the inner and outer segments (IS/OS) of the photoreceptors and the number of TdT-mediated dUTP nick-end labeling (TUNEL)-positive cells in the outer

nuclear layer (ONL) caused by light exposure were notably ameliorated by pramipexole. The effect of pramipexole was not eliminated by yohimbine pretreatment, suggesting that the protective effect of pramipexole on light-induced retinal damage was not result from alpha-2 adrenoceptor activation.

In the study of laser-induced CNV model, pramipexole was orally administered once a day for 7 days from the day of laser photocoagulation (100 μm spot size, 100 mW, 0.1 s duration). To evaluate the effect of ocular instillation of pramipexole, pramipexole solution was also applied to the cornea of rats 5 times a day for 7 days from the day of laser photocoagulation. Seven days after the laser photocoagulation, fluorescein angiography (FAG) was performed to evaluate the incidence of CNV. Both of oral administration and ocular instillation of pramipexole suppressed the CNV formation.

Having found that pramipexole was effective, I explored its potential mechanism using human retinal pigment epithelium ARPE-19 cell and hydroxyl radical scavenging activity assay in cell-free system. The cytoprotection of pramipexole was evaluated on H_2O_2-induced ARPE-19 cell injury, and pramipexole significantly suppressed H_2O_2-induced cell death without the promotion of cell proliferation. Furthermore, pramipexole significantly prevented H_2O_2-induced caspases-3/7 activation and the intracellular accumulation of reactive oxygen species (ROS) in ARPE-19 cells. Although pramipexole did not affect the activity of catalase and glutathione peroxidase, which are the antioxidant enzyme against H_2O_2, in ARPE-19 cells, it showed the direct scavenging activity toward a hydroxyl radical generated from H_2O_2 by the Fenton reaction.

The bromocriptine, a dopaminergic agonist, was also evaluated on light-induced retinal damage, laser-induced CNV, and H_2O_2-induced ARPE-19 cell injury, however, it did not show any protective effect. These results would indicate that retinal protective effect of pramipexole was not result from dopamine receptor activation.

My results suggested that pramipexole showed remarkable protection against light-induced retinal damage and laser-induced CNV, and this protection is likely through antioxidant effects, and it may be a novel and effective therapy for retinal degenerative disorders such as AMD.

List of Abbreviations

Abbreviation	Formula
4-HNE	4-hydroxynonenal
8OHdG	8-hydroxy-2-deoxyguanosine
8OHG	8-hydroxyguanine
ALS	Amyotrophic lateral sclerosis（筋萎縮性側索硬化症）
AMD	Age-related macular degeneration (加齢黄斑変性)
AREDS	Age-Related Eye Disease Study
ARVO	Association for Research in Vision and Ophthalmology
CNV	Choroidal neovascularization (脈絡膜血管新生)
DCFH-DA	2',7'-Dichlorodihydrofluorescin diacetate
ERG	Electroretinogram (網膜電図)
FAG	Fluorescein angiography (蛍光眼底造影)
GA	Geographic atrophy (地図状萎縮)
H&E	hematoxylin and eosin
IS/OS	Inner and outer segments (内節/外節)
MPTP	1-methyl-4-phenyl-1,2,3,6- tetrahydropyridine
NAC	N-acetyl-cysteine
ONL	Outer nuclear layer (外顆粒層)
PD	Parkinson’s disease (パーキンソン病)
RGC	Retinal ganglion cell (網膜神経節細胞)
ROS	Reactive oxygen species (活性酸素種)
RPE	Retinal pigment epithelium (網膜色素上皮)
SN	Substantia nigra (黒質)
TUNEL	TdT-mediated dUTP nick-end labeling
VEGF	Vascular endothelial growth factor (血管内皮細胞増殖因子)

Table of Contents

1. INTRODUCTION

The macula is the small part of the retina that is responsible for central vision, allowing us to see fine details clearly (Figure 1A and B). Age-related macular degeneration (AMD) is the most common cause of irreversible visual impairment of older adults in the developed world.[1, 2] Although the prevalence of AMD is increasing with the aging of the population, its etiology remains largely unclear. There are two major subtypes of AMD: the atrophic form, also called the dry type, and the neovascular form, also called the wet type. The former is characterized by geographic atrophy (GA) due to the death of the retinal pigment epithelium (RPE) and photoreceptor cells (Figure 1D),[3-5] and the latter develops due to choroidal neovascularization (CNV) (Figure 1E).[6] Although wet AMD can be treated by anti-vascular endothelial growth factor (VEGF) agents,[7, 8] there is no approved therapeutic treatment available for dry AMD. Moreover, novel wet AMD treatment is also eagerly anticipated because anti-VEGF drugs have shown a broad range of effective response on wet AMD.

Previous studies have shown that genetic, environmental, and behavioral factors are prominently involved in AMD development. [9-11] Increasing evidence has indicated a role of immune and inflammatory systems, particularly those in the complement system, in the pathogenesis of AMD. Investigations of genetic polymorphisms have identified the gene variant of complement components, such as complement factor H (CFH), factor B, and C3, as high risk factors for AMD.[12-16] An immunohistochemical study has revealed that drusen,

which is an accumulated waste material in aged retina, contains the complement proteins C3, C5, and C5b-9.[17] Because the complement system is a prominent part of inflammatory reactions, these findings have focused on the evidence of inflammation in the etiology of AMD. Furthermore, recent intensive studies have suggested that oxidative stress would be implicated in AMD pathogenesis. First, retinal photoreceptors are exposed to light daily; therefore, the retina is susceptible to oxidative damage caused by light-induced oxidation through photosensitizers in the photoreceptors.[18] Second, excessive accumulation of fluorescent lipofuscin, composition of drusen, in RPE cells is a hallmark of AMD,[19-21] and the lipofuscin isolated from human RPE shows substantial photoreactivity and can generate several reactive oxygen species (ROS), such as singlet oxygen, superoxide anion, and H_2O_2.[22] Third, during AMD, the iron level in the macula is significantly increased compared with healthy macula.[23] Iron is a known source of free radicals because it reacts with H_2O_2 in the Fenton reaction to generate a hydroxyl radical, which is the most reactive radical. Finally, there is evidence of increased oxidative damage in the retina of AMD patients, including widespread expression markers of lipid peroxidation, such as acrolein and 4-hydroxynonenal (4-HNE), markers of protein oxidation, such as nitrotyrosine, and indicators of DNA damage, such as 8-hydroxy-2-deoxyguanosine (8OHdG).[24] Therefore, drugs that can mitigate oxidative stress might produce beneficial effects for AMD.

Parkinson's disease (PD) is an age-related neurodegenerative disorder characterized by massive loss of dopaminergic neurons in the substantia nigra (SN).[25] Although the cause and pathogenesis of the disease still remain unclear, oxidative stress is considered to be associated with the loss of dopamine neurons.[26, 27] Namely, PD patients have a strong correlation to the dysfunction of complex I in mitochondria from SN, resulting excessive ROS.[28] PD is associated with increased level of nigral iron, producing most toxic ROS; hydroxyl radical.[29] Moreover, expression of 4-HNE was increased in nigral neuron from PD patients,[30] and 8-hydroxyguanine (8OHG), a marker of nucleoside oxidation, immunoreactive neurons corresponded to the distribution of neurodegeneration in SN of PD patients.[25] Although there is difference in source of ROS, we can find resemblance between AMD and PD in terms of involvement of oxidative damage in its pathogenesis.

Pramipexole dihydrochloride (abbreviated as pramipexole in this study), (S) -2-amino-4,5,6,7-tetrahydro-6-propylamino-benzothiazole dihydrochloride (Figure 2A), is a synthesized non-ergot dopamine receptor agonist that has been used to treat PD.[31] Previous studies have shown that pramipexole is a potent agonist at dopamine D2 receptor subfamily (D2, D3, and D4 receptor subtypes) with preferential affinity for the D3 receptor subtype, and demonstrably devoid of the affinity for dopamine D1 receptor.[32] Pramipexole also has an alpha2-adrenoceptor activity, but no other beta-adrenergic activity.[32] Pramipexole is well absorbed after the oral administration and its peak level in the plasma reaches within

approximately 2 h.[33] Bioavailability of pramipexole is more than 90%, and its protein binding in plasma is low.[33, 34] Pramipexole exerts its therapeutic effect on PD by restoring balance to dopamine signaling. In addition, several non-clinical studies have demonstrated that pramipexole has neuroprotective effects and that these effects resulted from its antioxidant activity.[35-39] Although the neuroprotective potential of pramipexole has been under intense investigation, to my knowledge, its retinal protective effect has not yet been investigated. Consistent with the hypothesis that an antioxidant would be effective on AMD, I investigated the potential of pramipexole as a new retinal protective agent.

To examine the possible use of pramipexole for retinal degenerative disorders such as AMD, I investigated its effect on light-induced retinal damage in mice, which is a model of dry AMD, and laser-induced CNV in rats, which is a model of wet AMD. Furthermore, I examined its antioxidant effect on H_2O_2-induced human RPE ARPE-19 cell injury and hydroxyl radical scavenging activity. I also evaluated bromocriptine (Figure 2B), other dopamine receptor agonist, on light-induced retinal damage in mice, laser-induced CNV in rats, and H_2O_2-induced ARPE-19 cell death.

2. MATERIALS and METHODS

2.1. Experimental Animals

All experiments were conducted according to the ARVO Statement for the Use of Animals in Ophthalmic and Vision Research, and were approved and monitored by the Institutional Animal Care and Use Committee of Santen Pharmaceutical Co., Ltd. Male BALB/c mice and BN/CrlCrlj rats (aged 8–9 weeks; Charles River Laboratories, Yokohama, Japan) were used for this study. All mice were housed in a specific pathogen-free facility maintained at 23°C ± 3°C on a 12 h light–dark cycle with free access to food and water.

2.2 Administration of test articles in mice: Study of light-induced retinal damage

2.2.1 Oral and intraperitoneal administration

Pramipexole dihydrochloride (Toronto Research Chemicals, Toronto, Canada) (Figure 2A) and bromocriptine mesilate (Sigma-Aldrich, St. Louis, MO, USA) (Figure 2B) were orally administered (consistent with clinical use) 1 h before light exposure. Yohimbine hydrochloride (Sigma-Aldrich, St. Louis, MO, USA) was intraperitoneally injected 0.5 h prior to the pramipexole treatment based on a previous study.[40] For administration, 1% methylcellulose solution and physiological saline (Otsuka pharmaceutical factory, Tokushima, Japan) were used as the vehicle for oral treatments and intraperitoneal injections, respectively.

2.2.2. Ocular instillation

One μL of pramipexole solution was applied to cornea with 5 times a day every 1.5 h for 2 days from the day before the light exposure. For administration, physiological saline was used as the vehicle.

2.3. Administration of test articles in rat: Study of laser-induced CNV

2.3.1. Oral administration

Pramipexole dihydrochloride and bromocriptine mesilate were orally administered once a day for 7 days from the day of laser photocoagulation. On the day of laser photocoagulation, test articles were administrated just before the laser treatment. For administration, 1% methylcellulose solution was used as the vehicle.

2.3.2. Ocular instillation

Five μL of pramipexole solution was applied to cornea with 6 times a day every 1.5 h for 7 days from the day of laser photocoagulation. For administration, physiological saline was used as the vehicle.

2.4. Light exposure in mice

Light exposure was performed as previously described.[41] The mice were kept in total darkness for 24 h. One drop of 0.5% tropicamide and 0.5% phenylephrine hydrochloride

(Santen, Osaka, Japan) was applied to the cornea for pupillary dilation 1 h before light exposure. The mice were exposed to 5000 lux of white fluorescent light for 2 h in a light exposure box with laterally placed mirrors. Immediately after light exposure, the mice were maintained in total darkness for 24 h (Figure 3).

2.5. Electroretinogram of light-induced retinal damage model

Electroretinogram (ERG) analysis was conducted as previously described.[42] In brief, ERGs were recorded using a Portable ERG&VEP LE-3000 (Tomey, Nagoya, Japan) 24 h after the light exposure (Figure 3). The dark-adapted mice were anesthetized with an intramuscular injection of ketamine (45 mg/kg body weight; Daiichi-Sankyo, Tokyo, Japan) and xylazine (2.5 mg/kg body weight; Bayer Health Care, Leverkusen, Germany). One drop of 0.5% tropicamide and 0.5% phenylephrine hydrochloride was applied to the cornea, and one drop of 0.4% oxybuprocaine hydrochloride (Santen, Osaka, Japan) was applied for local anesthesia. The corneal electrode was mounted on the center of the cornea. The reference and ground electrodes were subcutaneously placed in nose and tail, respectively. A single light-flash stimulus (3000 cd/m^2 for 10 ms) was applied to the eye using an LED lamp through the corneal electrode. This ERG recording process was conducted under dim red light, and the mice were kept warm during the process. The amplitude of the a-wave was defined as the distance from the baseline to the maximum peak of the a-wave, and the amplitude of the

b-wave was defined as the distance from the maximum peak of the a-wave to the maximum peak of the b-wave (Figure 4).

2.6. Histopathological Analysis of light-induced retinal damage model

The mice were humanely euthanized by abdominal aorta excision under the anesthesia by an intraperitoneal injection of sodium pentobarbital (80 mg/kg body weight; Sumitomo-Dainippon, Osaka, Japan) 24 h after light exposure. Immediately after euthanization, the eyes were enucleated, fixed with 4% paraformaldehyde/0.1 M phosphate buffer overnight at room temperature, dehydrated in a graded ethanol series, and embedded in paraffin. Mid-sagittal sections were prepared for hematoxylin and eosin (H&E) and TdT-mediated dUTP nick-end labeling (TUNEL) staining. TUNEL staining was performed by using the *in situ* Apoptosis Detection Kit (Takara Bio, Shiga, Japan). Histopathological findings were visualized and photographed by the NanoZoomer (Hamamatsu Photonics, Shizuoka, Japan). Previous studies have shown that apoptotic cell death caused by excessive light exposure can be visualized in the outer nuclear layer (ONL) of the retina using TUNEL staining, and the number of TUNEL-positive cells was counted to evaluate the protective effect of experimental compounds. [43-45] In this study, the TUNEL-positive cells in the ONL were counted from the area between 200 and 800 μm superior to the optic disc.

2.7. Laser-induced CNV in rat

CNV was induced by laser photocoagulation-induced rupture of Bruch's membrane as previously described.[46] In brief, 1 drop of 0.5% tropicamide and 0.5% phenylephrine hydrochloride was applied to the cornea of rats for pupillary dilation. Rats were anesthetized with an intramuscular injection of ketamine (45 mg/kg body weight) and xylazine (2.5 mg/kg body weight). Eight burns of laser photocoagulation (100 μm spot size, 100 mW, 0.1 s duration) were applied between the major retinal vessels close to the optic disc using MC-300 Multicolor Laser Photocoagulator System (Nidek, Aichi, Japan) (Figure 5A).

2.8. Fluorescein angiography (FAG) of laser-induced CNV model

Seven days after the laser photocoagulation, the presence of CNV was confirmed by fluorescein angiography (FAG) as described before (Figure 6).[47] In brief, 1 drop of 0.5% tropicamide and 0.5% phenylephrine hydrochloride was applied to the cornea of rats for pupillary dilation, and then rats were anesthetized with an intramuscular injection of ketamine (45 mg/kg body weight) and xylazine (2.5 mg/kg body weight). The 10 % fluorescein (Alcon japan, Tokyo, Japan) was injected into tail vein of the anesthetized rats, and fluorescein angiograms were obtained by means of a fundus camera PROIII (Kowa, Nagoya, Japan) (Figure 5B). The incidence of CNV at each eye was calculated by following formula.

Formula; Incidence of CNV (%) = number of CNV spot / number of laser burn spot x100

2.9. Cell Culture

Human retinal pigment epithelium(RPE) RPE-19 cells (CRL-2302; American Type Culture Collection, Manassas, VA, USA) were cultured in Dulbecco's Modified Eagle's Medium Nutrient Mixture F-12 (Nacalai Tesque, Kyoto, Japan) supplemented with 10% fetal bovine serum (Biowest, Caille, France) and 100 U/mL penicillin-100 µg/mL streptomycin (Gibco, Grand Island, NY, USA) at 37°C in a humidified 5% CO_2 incubator, as previously described.[48]

2.10. Cell Viability Assay

Following a 3 h co-treatment with 250 µM H_2O_2 (Wako Pure Chemicals, Osaka, Japan) and test article, a cell viability assay was performed. The cells were pre-treated with the test article 24 h prior to the H_2O_2 stimulation. Cell viability was quantified using a Cell Counting Kit-8 (Dojindo, Kumamoto, Japan) in accordance with manufacturer's protocol. The procedures used have been described elsewhere.[49] In brief, the medium was replaced with fresh medium containing WST-8 reagent from the kit, and the plate was incubated at 37°C in a humidified 5% CO_2 incubator for 1.5 h. Absorbance at 450 nm was measured using a benchmark plus microplate reader (Bio-Rad, Hercules, CA, USA) to determine the relative number of viable

cells. Furthermore, to evaluate the effect of pramipexole on cell proliferation, cell viability was quantified, following the treatment with pramipexole alone for 27 h.

2.11. Caspase-3/7 Activity Assay

Following a 3 h co-treatment with 250 μM H_2O_2 and test article, the activities of caspases-3/7 were determined. The cells were treated with pramipexole 24 h prior to the H_2O_2 stimulation. Caspase-3/7 activity was measured using the Caspase-Glo 3/7 assay kit (Promega, Fitchburg, WI, USA) in accordance with the manufacturer's protocol. The procedures used have been described in a previous study.[50] In brief, the Caspase-Glo 3/7 reagent was added to each well, and the contents of the wells were gently mixed with a plate shaker for 30 s. The plate was then incubated at room temperature for 0.5 h. Luminescence was measured using the EnVision multilabel reader (PerkinElmer, Waltham, MA, USA).

2.12. Intracellular ROS Assay

An intracellular reactive oxygen species (ROS) assay was performed using the cell-permeable fluorogenic probe 2′,7′-dichlorodihydrofluorescin diacetate (DCFH-DA) of the OxiSelect intracellular ROS assay kit (Cell Biolabs, San Diego, CA, USA) in accordance with the manufacturer's protocol. The procedures have been described elsewhere.[38, 51] DCFH-DA penetrates into cells and is converted by an intracellular esterase into non-fluorescent DCFH,

which reacts with ROS to form the highly fluorescent DCF. Therefore, the fluorescence intensity correlates with intracellular ROS levels. Following a 24 h treatment with pramipexole, the cell medium was replaced with medium containing DCFH-DA, and the plate was incubated at 37°C in a humidified 5% CO_2 incubator for 15 min. The medium was replaced with fresh medium containing pramipexole and 250 μM H_2O_2. After a 3 h incubation, intracellular ROS accumulation was visualized, imaged, and quantified using an Axiovert 200 M inverted microscope, AxioVision Viewer (Carl Zeiss, Oberkochen, Germany), and EnVision multilabel reader, respectively. Fluorescence intensity was determined using an excitation wavelength of 485 nm and an emission wavelength of 535 nm.

2.13. Catalase and Glutathione Peroxidase Activity Assay

Catalase and glutathione peroxidase activity assay was performed using catalase assay kit and glutathione peroxidase assay kit (Cayman chemical, Ann Arbor, MI, USA) in accordance with the manufacturer's protocol. After the treatment with pramipexole or vehicle for 27 h, ARPE-19 cells were lysed in proper lysate buffers according to each assay's protocol. Catalase assay is based on the reaction of the enzyme with methanol in the presence of H_2O_2. The formaldehyde, which is oxidative product of methanol, is measured by colorimetric analysis using 4-amino-3-hydrazino-5-mercapto-1,2,4- triazole, and it is directly proportional to the catalase activity. Absorbance at 540 nm was measured using a benchmark plus

microplate reader to determine the catalase activity. Glutathione peroxidase assay is based on coupled reaction with glutathione reductase. Oxidized glutathione, which is produced by glutathione peroxidase, is recycled by glutathione reductase and NADPH. The oxidation of NADPH to $NADP^+$ caused by this recycle reaction decreases the absorbance at 340 nm. The rate of decrease of absorbance represents the glutathione peroxidase activity. Absorbance at 340 nm was measured using a benchmark plus microplate reader.

2.14. Hydroxyl Radical Scavenging Activity Assay

Hydroxyl radical scavenging activity was measured using the OxiSelect Hydroxyl Radical Antioxidant Capacity (HORAC) Activity Assay Kit (Cell Biolabs, San Diego, CA, USA) in accordance with manufacturer's protocol. The procedures used have been described previously.[52] The hydroxyl radical generated by the Fenton reaction oxidizes and quenches the fluorescein probe, forming the basis of this assay. Namely, the antioxidant capacity of the experimental compound correlates with the fluorescence decay curve, and the area under the curve (AUC) of the fluorescence decay curve was used to quantify the hydroxyl radical scavenging activity of the test compound. The activity was normalized to the concentration of gallic acid, which was used as an antioxidant standard in this assay. The intensity of fluorescein was measured using EnVision multilabel reader (excitation, 485 nm; emission, 535 nm) every 5 min for a total of 60 min.

2.15. Data Analysis

The values are expressed as the mean ± SEM. All experiments were conducted in at least quadruplicate. The data from two groups were analyzed using Student's *t*-test or Aspin Welch's *t*-test, whereas data from multiple groups were analyzed using an ANOVA followed by Dunnett's multiple comparison test. Values of $P < 0.05$ were considered significant.

3. RESULTS

3.1. Pramipexole and light-induced retinal dysfunction

The effect of pramipexole on light-induced retinal dysfunction was investigated using ERG analysis. Representative ERG waves are shown in Figure 7. The amplitudes of the a- and b-wave of the ERG were markedly reduced in vehicle-treated mice after light exposure (Figure 7B) compared with normal mice (Figure 7A). Treatment with pramipexole (0.1 and 1 mg/kg body weight) diminished the light-induced decrease in the amplitudes of the a- and b- wave in a dose-dependent manner (Figure 7C and D).

The quantitative analyses of the a- and b-wave amplitudes of the ERGs are shown in Figure 8A and 8B, respectively. Light exposure to vehicle-treated mice significantly reduced the amplitudes of the a-wave (41 ± 15 μV) and b-wave (78 ± 30 μV) compared with vehicle-treated mice without light exposure (303 ± 26 μV and 593 ± 44 μV for a- and b-wave amplitudes, respectively). In the light-exposed mice, administration of pramipexole (0.1 and 1 mg/kg body weight) diminished the decrease of the a- and b-wave amplitude in a dose-dependent manner. These effects were significant at 0.1 and 1 mg pramipexole/kg body weight.

3.2. Pramipexole and light-induced photoreceptor degeneration

To confirm the protective effects of pramipexole, morphologic studies were performed at 24 h after light exposure. Images of typical H&E staining of the retina are shown in Figure 9A-D. In the retina of vehicle-treated mice with light exposure (Figure 9B), the inner and outer segments (IS/OS) of photoreceptors and the external limiting membranes were destroyed, the shape of the ONL was irregular, and the RPE cells were swelled compared with the retinas of normal mice (Figure 9A). Treatment with pramipexole (0.1 and 1 mg/kg body weight) suppressed these retinal changes in a dose-dependent manner (Figure 9C and D). Figure 9E-H shows representative images of the retina with TUNEL staining, which reveals apoptotic cell death. Figure 9I shows the quantitative analysis of the number of TUNEL-positive cells in ONL. The number of TUNEL-positive cells was significantly increased in vehicle-treated mice after light exposure compared with those without light exposure (2.0 ± 1.7 cells and 119.3 ± 26.9 cells without and with light exposure, respectively). Treatment with pramipexole (0.1 and 1 mg/kg body weight) significantly reduced the number of TUNEL-positive cells compared with vehicle-treated mice with light exposure in a dose-dependent manner.

3.3. Ocular instillation of Pramipexole and light-induced retinal dysfunction

To explore the topical administration route of pramipexole, the effect of eye-drop of pramipexole were evaluated on light-induced retinal dysfunction using ERG analysis. The

quantitative analyses of the a- and b-wave amplitudes of the ERGs are shown in Figure 10A and 10B, respectively. Light exposure to vehicle-treated mice significantly reduced the amplitudes of the a-wave (159 ± 13 μV) and b-wave (290 ± 29 μV) compared with vehicle-treated mice without light exposure (449 ± 40 μV and 883 ± 82 μV for a- and b-wave amplitudes, respectively). In the light-exposed mice, treatment with eye-drop of pramipexole (0.006, 0.02, 0.06, and 0.2%) inhibited the light-induced retinal dysfunction. The effect of pramipexole was statistically significant at concentration of 0.02% and 0.2% in a-wave, and all concentrations in b-wave.

3.4. Bromocriptine and light-induced retinal dysfunction

Bromocriptine is a dopamine receptor agonist used as treatment for PD along with pramipexole. To validate whether the protective effect of pramipexole resulted from dopamine receptor agonistic activity, the effect of bromocriptine on light-induced retinal dysfunction was evaluated using ERG analysis. Representative ERG waveforms are shown in Figure 11A. The quantitative analyses of the a- and b-wave amplitudes of the ERGs are shown in Figure 11B and 11C, respectively. Treatment of bromocriptine (0.1 and 1 mg/kg body weight) to light-exposed mice did not show a protective effect compared with vehicle-treated mice with light exposure.

3.5. Yohimbine and its impact on the protective effect of pramipexole

Pramipexole combines dopamine receptor agonist and alpha-2 adrenoceptor agonist activity.[32] To evaluate the contribution of alpha-2 agonist activity to the retinal protective effect of pramipexole, the influence of yohimbine, an alpha-2 adrenoceptor antagonist, on the retinal protection of pramipexole was evaluated using ERG analysis. The quantitative analyses of the a- and b-wave amplitudes of the ERGs are shown in Figure 12A and 12B, respectively. As with the former data (Figure8), treatment of pramipexole (1 mg/kg body weight) to light-exposed mice significantly prevented the decrease in the a-and b-wave amplitudes of the ERGs compared with vehicle-treated mice with light exposure. Treatment with yohimbine (10 mg/kg body weight) prior to pramipexole did not affect the a- and b-wave recovery.

3.6. Pramipexole and laser-induced CNV

To evaluate the ability of pramipexole as a treatment for wet AMD, I investigated the effect of the oral administration of pramipexole on laser-induced CNV in rat. Seven days after laser burn, CNV formation at each laser photocoagulation spot was evaluated by FAG, and the efficacy of experimental compound was described by the incidence of CNV. The result is shown in Figure 13. The incidence of CNV in vehicle-treated rats with laser photocoagulation

was 71.9 ± 4.6%. In the rats orally administrated pramipexole (0.1 and 1 mg/kg body weight), the incidence of CNV was significantly reduced in a dose-dependent manner.

3.7. Ocular instillation of pramipexole and laser-induced CNV

To evaluate the effect of pramipexole administered through ocular instillation, the pramipexole solution was applied to the cornea of laser-induced CNV model in rat, and the result is shown in Figure 14. The incidence of CNV in vehicle-treated rats with laser photocoagulation was 71.9 ± 3.9%, and pramipexole eye-drops reduced the incidence of CNV. The effect of pramipexole was statistically significant at concentration of 1%.

3.8. Bromocriptine and laser-induced CNV

To validate whether the anti-CNV effect of pramipexole resulted from dopamine receptor agonistic activity, the effect of bromocriptine with oral administration was evaluated on laser-induced CNV model. The result is shown in Figure 15. The incidence of CNV in vehicle-treated rats with laser photocoagulation was 75.0 ± 3.3%. In the rats orally administrated bromocriptine (0.3, 1, and 3 mg/kg body weight), there was no significant difference in incidence of CNV compared with vehicle-treated rats.

3.9. Pramipexole, bromocriptine and H_2O_2-induced ARPE-19 cell death

To clarify the potential of pramipexole and bromocriptine against oxidative damage, their effect on H_2O_2-induced ARPE-19 cell death was evaluated. Figure 16A and 16B shows the results with pramipexole and bromocriptine, respectively. The values are expressed as a percentage of the untreated control group. Incubation with 250 μM H_2O_2 significantly reduced the cell viability to 55.7% ± 3.6% of control. Various concentrations of pramipexole (10^{-8} to 10^{-3} M) suppressed H_2O_2-induced cell death in a concentration-dependent manner (Figure 16A). The effect of pramipexole was significant at concentrations of 10^{-6} M or more. In contrast, bromocriptine showed no protective effect at concentrations from 10^{-10} to 10^{-6} M (Figure 16B). Moreover, effect of pramipexole on cell proliferation was evaluated because the proliferative effect that can increase relative living cell numbers after H_2O_2 treatment. Pramipexole up to 10^{-3} M did not increase the number of cells (Figure 17). This result indicated that the cytoprotection of pramipexole was not a result of increased cell proliferation.

3.10. Pramipexole and H_2O_2-induced caspase-3/7 activation

To examine the anti-apoptotic effect of pramipexole, the effect of pramipexole on H_2O_2-induced activation of caspases-3/7, which act as final effectors of apoptotic cell death, was evaluated, and the result is shown in Figure 18. The values are expressed as a percentage of the untreated control group. Incubation with 250 μM H_2O_2 for 3 h significantly stimulated

caspase-3/7 activity in ARPE-19 cells to 133.5% ± 4.4% of control levels. Treatment with pramipexole (10^{-5} to 10^{-3} M) significantly suppressed this activation in a concentration-dependent manner. Treatment with pramipexole alone did not significantly influence caspase-3/7 activity compared with that of controls.

3.11. Pramipexole and H_2O_2-induced intracellular ROS accumulation

Because a recent report suggested that excessive intracellular ROS accumulation initiates the apoptotic machinery,[53] I next investigated the effect of pramipexole on H_2O_2-induced intracellular ROS accumulation. Typical images of ARPE-19 cells are shown in Figure 19A-L. Quantitative analysis of the fluorescent intensity, which is proportional to the intracellular ROS level, is shown in Figure 19M. The values are expressed as a percentage of untreated control cells. Incubating cells with 250 μM H_2O_2 for 3 h significantly induced ROS accumulation to 290.5% ± 3.0% of controls. The addition of pramipexole (10^{-5} to 10^{-3} M) significantly reduced ROS levels in a concentration-dependent manner. Treatment of pramipexole alone slightly, but significantly, increased ROS levels compared with that of control.

3.12. Pramipexole and antioxidant enzyme

To evaluate the effect of pramipexole on antioxidant enzyme in ARPE-19, the catalase and glutathione peroxidase activity, which catalyze the reduction of H_2O_2, were measured. Figure 20A and 20B shows the results of catalase activity and glutathione peroxidase activity, respectively. Values are expressed as percentage of control, which was the untreated cell group. Incubation with pramipexole (10^{-5} to 10^{-3} M) for 27 h did not influence the activity of catalase and glutathione peroxidase in ARPE-19 cells.

3.13. Pramipexole and Hydroxyl radical

To evaluate the hydroxyl radical scavenging activity of pramipexole, a HORAC activity assay was performed. Figure 21 shows the HORAC activity of pramipexole normalized to the concentration of gallic acid, which is the antioxidant standard in this assay. Pramipexole had direct scavenging activity toward the hydroxyl radical, and the activity was increased in a concentration-dependent manner. This evidence suggests that pramipexole prevents hydroxyl radical-induced oxidative damage.

4. DISCUSSION

A neuroprotective effect of pramipexole, a therapeutic agent for PD, has previously been shown in various neuronal cells and animal models of central neurological disorders.[35-39, 54-57] However, to my knowledge, no study has evaluated the effect of pramipexole on retinal damage. My present study revealed that pramipexole had a beneficial effect on light-induced retinal damage in mice and laser-induced CNV in rats.

Light-induced retinal damage in animals has been used as a model to investigate new therapeutic agents for retinal degenerative disorders, such as dry AMD. [43-45, 58, 59]. Excessive light exposure is cited as a risk factor for onset and progression of AMD,[60] and light-induced retinal damage in animals results from oxidation-induced apoptosis, which has similarly been found in dry AMD patients.[24, 61] Excessive exposure to light is well known to cause retinal dysfunction in animals and is represented by a decrease in the a- and b-wave amplitudes on ERG.[43-45] Therefore, I first evaluated the effect of pramipexole on light-induced retinal dysfunction using ERG. For *in vivo* studies, the neuroprotective effect of pramipexole has been demonstrated in post-ischemic- or methamphetamine-induced nigrostriatal degeneration mouse models at a dose of 1 mg/kg body weight (p.o.).[62] Hence, doses of 0.1 and 1 mg/kg body weight were used in this study. Vehicle-treated mice had a significant decrease in the ERG a- and b-wave amplitudes after light exposure, and pramipexole significantly prevented light-induced retinal dysfunction in a dose-dependent manner (Figure 7 and 8).

To confirm these electrophysiological data, I performed morphologic studies. According to previous reports, photoreceptors suffer remarkable damage from excessive light exposure, whereas the inner retinal structures are preserved.[43-45] It has also been reported that apoptotic cell death is recognized as the primary cause of photoreceptor death after light exposure, and the number of TUNEL-positive cells in the ONL, which is the cell body of the photoreceptor, was counted to evaluate the protective effect of experimental compounds.[43-45] In this study, the number of TUNEL-positive cells in the ONL significantly increased in vehicle-treated mice after light exposure, and treatment with pramipexole diminished the number of TUNEL-positive cells in a dose-dependent manner (Figure 9). In addition, I explored the topical administration route of pramipexole due to having the expectation to avoid the systemic side effects such as somnolentia in considering the use in human. In this study, ocular instillation of pramipexole showed the protective effect against light-induced retinal dysfunction, however, the efficacy was weaker than that of oral administration (Figure 10). These findings suggest that pramipexole can suppress photoreceptor cell death caused by light exposure and ameliorate the impaired visual function.

A similar neuroprotective effect of pramipexole has been observed in various animal models of PD. [37, 39, 57, 62] For example, in the rotenone-induced mouse model of PD, pramipexole was shown to protect against dopaminergic neuronal cell death in the SN and against motor system dysfunction.[37] Similarly, pramipexole attenuated dopaminergic neuronal loss in the

SN in the 1-methyl-4-phenyl-1,2,3,6- tetrahydropyridine (MPTP)-induced mouse model of PD.[39] Although the affected region is different between PD and AMD models, my results that pramipexole has a retinal protective effect are consistent with findings from these earlier studies.

Bromocriptine is classified into a dopaminergic agonist, and it has been used as a treatment for PD as with pramipexole.[63] In an *in vivo* study, bromocriptine (1 mg/kg body weight) showed an effect to restore the balance to the dopamine receptor on rats with 6-hydroxydopamine lesions.[64] According to this study, doses of 0.1 and 1 mg/kg body weight of bromocriptine were used in this study. Unlike pramipexole, however, bromocriptine did not show a protective effect against light-induced retinal dysfunction in the present study (Figure 11). *In situ* hybridization analysis of the distribution of dopamine receptor subtypes in the rat retina has revealed that the expression of dopamine receptors D2 and D3, which are targets of pramipexole, were not observed in photoreceptors.[65] In addition, previous studies reported that pramipexole protected neural cells through the mechanism independent of dopamine D2/D3 receptors.[35, 36] Consequently, the protective effect of pramipexole on photoreceptors might not result from dopamine receptor activation.

Pramipexole also has alpha-2 adrenoceptor agonist activity[32], and there are several lines of evidence that alpha-2 adrenoceptor agonist brimonidine shows protective effect on retinal neuronal damage. For instance, brimonidine significantly increased retinal ganglion cells

(RGC) survival after transient retinal ischemia induced by ligature of the ophthalmic vessels or acute intraocular pressure elevation[40, 66]. Furthermore, brimonidine decreased Bax which is pro-apoptotic member of Bcl-2 family that plays principle role in apoptosis pathway but increased expression of anti-apoptotic factors such as Bcl-xL and phosphorylated Bad in ischemic retina[66]. To confirm the influence of alpha-2 adrenoceptor agonist activity of pramipexole on its retinal protective effect, the effect of combination treatment with yohimbine, specific alpha-2 adrenoceptor antagonist, and pramipexole was evaluated on light-induced retinal damage model in this study. The pretreatment of yohimbine was designed based on previous study[40]. Briefly, intraperitoneal injection of yohimbine (5 mg/kg body weight) at 20 minutes before the treatment of brimonidine has prevented the protective effect of brimonidine on ischemia-induced RGC death. However, my data showed that the protective effect of pramipexole is not affected by yohimbine suggesting that retinal protective effect of pramipexole would not be mediated via alpha-2 adrenoceptor (Figure 12).

Laser-induced CNV in animal has been widely used as a model of wet AMD,[47, 67-69] because the animal models are able to mimic the CNV, which is a primary feature of wAMD.[6] It has been reported that intravitreal injection of aflibercept, launched anti-VEGF drug for wet AMD, suppressed the CNV formation in laser-induced CNV model in mice,[67] indicating that the laser-induced CNV model reflects the pathogenesis of wet AMD, and proves the validity of disease model for wet AMD. In both laser-induced CNV model and wet AMD patients, the

CNV has been observed using fluorescein angiography.[6, 67] Since the tight junction of CNV is weak, the leakage of fluorescein in retina reveals the presence and form of CNV. In this study, oral administration of pramipexole significantly prevented the CNV formation in a dose-dependent manner (Figure 13). Ocular instillation of pramipexole has also shown the inhibitory effect on CNV formation (Figure 14), however, the efficacy was weaker than that of orally administered pramipexole in common with the former result of light-induced retinal dysfunction. Probably, oral administration is better than ocular instillation in terms of drug distribution in retina for pramipexole. In contrast, bromocriptine showed no inhibitory effect on laser-induced CNV model in accordance with former study on light-induced retinal damage in mice (Figure 15). Therefore, the inhibitory effect of pramipexole on CNV formation would not result from dopamine receptor agonist activity.

In animals exposed to excessive light, H_2O_2 production was increased in the ONL,[70] and expressions of 4-HNE, 4-hydroxyhexenal, and 8OHdG, which are markers for oxidative damage, were increased in the retina.[45, 71] Moreover, the retinal damage caused by light exposure was ameliorated by treatment with antioxidants such as edaravone, N-acetyl-cysteine, and phenyl- N-tert-butylnitrone.[43, 45, 58, 59] Similarly, retina of laser-induced CNV model increased the ROS and 4-HNE level, and potent antioxidants such as apocynin, NADPH oxidase inhibitor, and NAC normalized these oxidative markers and suppressed the CNV formation.[69, 72] Although the exact cause of AMD is still unknown, oxidative stress

likely plays an important role in its pathogenesis.[18, 24, 73, 74] For instance, excessive accumulation of fluorescent lipofuscin in RPE represents a characteristic finding of AMD.[19-21] This accumulation is cited as one of the causes of AMD because the lipofuscin is able to generate several ROS such as singlet oxygen, superoxide anion, and H_2O_2.[22] Consequently, oxidative damage is considered to be involved in pathogenesis of AMD in humans, light-induced retinal damage, and laser-induced CNV in animals. Pramipexole has a demonstrated protective effect against oxidative stress-induced neuronal cell death.[35, 36] A previous study has shown that H_2O_2-induced rat pheochromocytoma PC12 cell death was inhibited by pramipexole at a concentration of 10^{-4} M.[36] A protective effect of pramipexole on MPP^+, the active metabolite of MPTP, -induced human neuroblastoma SH-SY5Y cell death has also been reported at concentrations from 3 x 10^{-4} to 3 x 10^{-3} M.[35] To investigate the antioxidant ability of pramipexole in retinal cells, I evaluated the effect of pramipexole on H_2O_2-induced human RPE ARPE-19 cell death using concentrations from 10^{-8} to 10^{-3} M and found that pramipexole protected against ARPE-19 cell death in a concentration-dependent manner (Figure 16A). This finding is in accordance with previous reports[35, 36] and also suggests that pramipexole exerts antioxidant properties in retinal cells as well as in neuronal cells. In contrast, bromocriptine did not show any cytoprotection (Figure 16B). The lack of antioxidant ability would be the reason for the null effect of bromocriptine on light-induced retinal damage in mice and laser-induced CNV in rats.

Previous studies have suggested that the pro-apoptotic molecule cytochrome *c* is released from the mitochondria and activates the complex of Apaf-1 and caspase-9, leading to the activation of caspases-3/7, which are the final effectors in the apoptotic pathway.[75, 76] It has been reported that H_2O_2-induced cytochrome *c* release from mitochondria was inhibited by pramipexole in SH-SY5Y and PC12 cells.[36, 54] In this study, I examined the ability of H_2O_2 to activate caspase-3/7 in ARPE-19 cells and then investigated the effect of pramipexole on this H_2O_2-induced effect. I found that pramipexole inhibited H_2O_2-induced activation of caspase-3/7 in a concentration-dependent manner (Figure 18). This finding indicates that the H_2O_2-induced ARPE-19 cell death is apoptotic as is the case in photoreceptor cell death after the light exposure to the animals, and pramipexole inhibits the apoptotic cell death caused by oxidative stress.

Catalase and glutathione peroxidase are ubiquitous antioxidant enzymes, and catalyze the reduction of H_2O_2 to protect the cells from oxidative damage. In this study, I evaluated the effect of pramipexole on the activity of catalase and glutathione peroxidase in ARPE-19 cell, however, the activities of them were not affected by the treatment of pramipexole (Figure 20), indicating that the antioxidative effect of pramipexole was not a result from up-regulation of antioxidant enzyme activity.

In this study, pramipexole suppressed H_2O_2-induced intracellular ROS accumulation in ARPE-19 cells (Figure 19) and showed scavenging activity on hydroxyl radical generated

from H_2O_2 by the Fenton reaction in a concentration-dependent manner (Figure 21). Recently, it was reported that increases in cytoplasmic ROS lead to the depletion of the mitochondrial membrane potential in cooperation with Ca^{2+}, resulting in the release of cytochrome *c* into the cytoplasm and activation of apoptosis.[53] A previous study demonstrated that excessive light exposure induced the production of H_2O_2 in the ONL.[70] Although the oxidizing capacity of H_2O_2 is weak, it can easily change to a hydroxyl radical by reacting with metals, including iron, in living organisms. Hydroxyl radical is the most reactive ROS and inflicts severe damage on cellular constituents such as lipids, proteins, and DNA. Therefore, suppression of hydroxyl radical would prevent oxidative damage. In fact, edaravone can scavenge hydroxyl radical, protecting against photoreceptor cell death after light exposure.[45, 77] Taken together, the key factor that contributes to the retinal protective effect of pramipexole in this study could be its potent ability to scavenge hydroxyl radical.

In conclusion, pramipexole showed remarkable protection against light-induced retinal damage and laser-induced CNV, and this protection is likely through antioxidant effects. Randomized and placebo-controlled clinical trials as part of the Age-Related Eye Disease Study (AREDS) suggested that antioxidant supplementation (vitamins C and E and beta carotene) reduces the odds of developing advanced AMD,[78] suggesting that antioxidants might be promising treatments for AMD. The administration of pramipexole to amyotrophic lateral sclerosis (ALS) patient reduces the serum level of 2,3-dihydroxybenzoic acid, a marker

for free radical activity,[79] indicating that pramipexole has antioxidant effects in humans. Because of the proven clinical pharmacokinetic and safety profile of pramipexole, my present results suggest a possible clinical use of pramipexole for the treatment of retinal degenerative disorders such as AMD.

5. ACKNOWLEDGMENTS

I would like to express my sincere gratitude to my supervisor, Professor Kenji Kohno (Nara Institute of Science and Technology), Dr. Masatsugu Nakamura, and Dr. Kazuyoshi Okamoto (Santen Pharmaceutical Co., Ltd.) for critical guidance and counseling of this research. I am very grateful to Dr. Osamu Katsuta, Ms. Sayo Habashita-Obata, and Ms. Asuka Sakamoto-Kamimura (Santen Pharmaceutical Co., Ltd.) for their valuable cooperation in pathological investigation, *in vivo* study, and *in vitro* study, respectively. Finally, I would like to offer my special thanks to my family; Mai Shibagaki, Aoi Shibagaki, and Nichika Shibagaki, for their understanding, support, and sacrifice during my study.

6. FIGURES

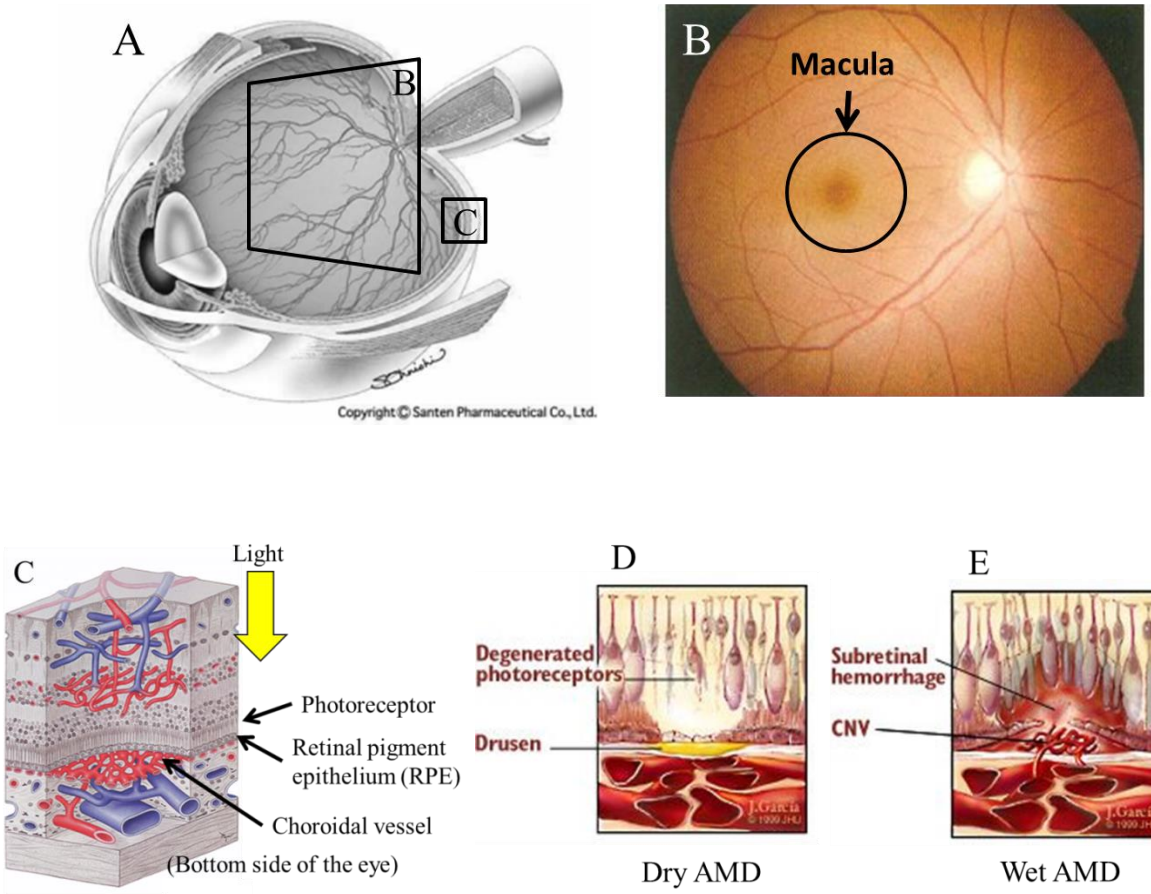

Figure 1 Anatomical chart images of the eye and disease states

Ocular globe (A), Fundus photograph (B), Retinal cell layers (C), Diagram of dry AMD (D) and wet AMD (E)

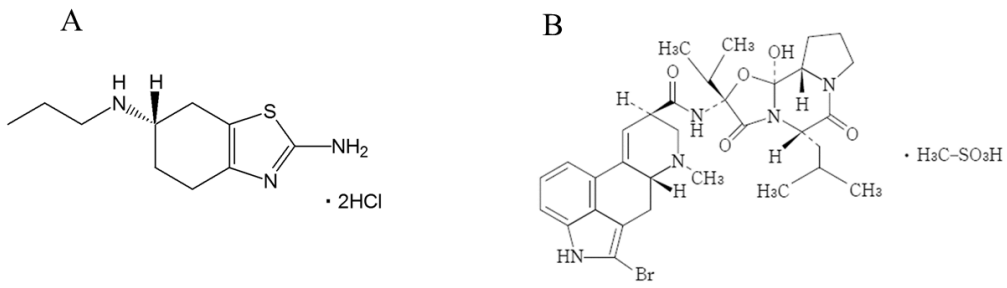

Figure 2 Chemical structures of pramipexole (A) and bromocriptine (B)

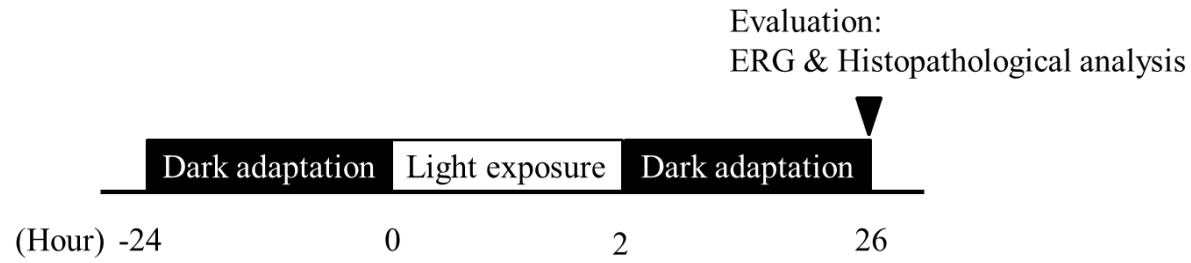

Figure 3 Timeline of study of light-induced retinal damage in mice, including induction of impairment and evaluation

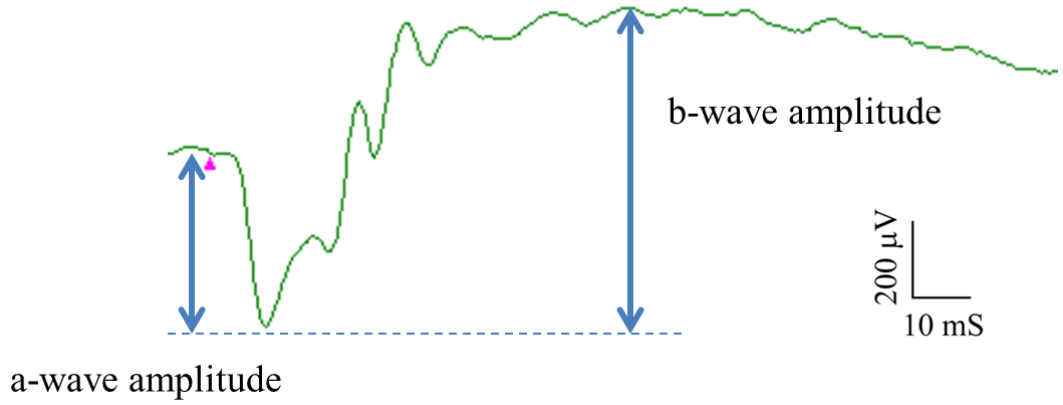

Figure 4 ERG wave

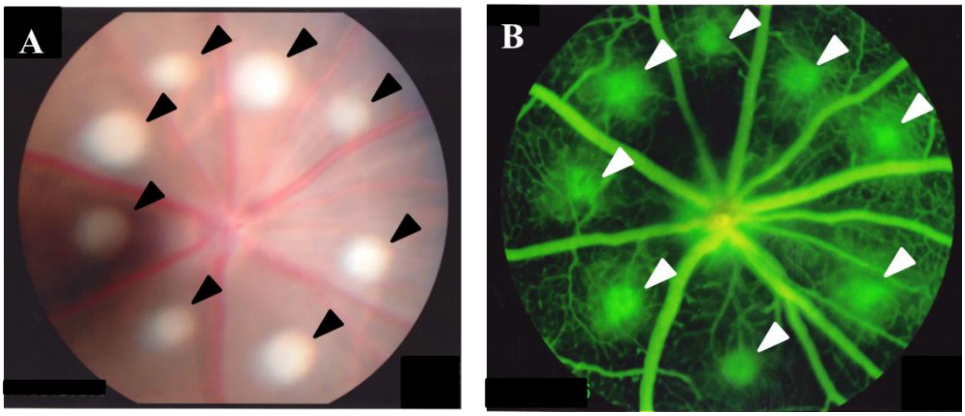

Figure 5 Representative fundus images of laser-induced CNV model in rat

Collar fundus image obtained just after the laser photocoagulation (A) Black allow heads indicate the laser burn spots. Fluorescein angiography image of retina obtained 7 days after the laser photocoagulation (B) White allow heads indicate the leakage of fluorescein, suggesting the presence of CNV.

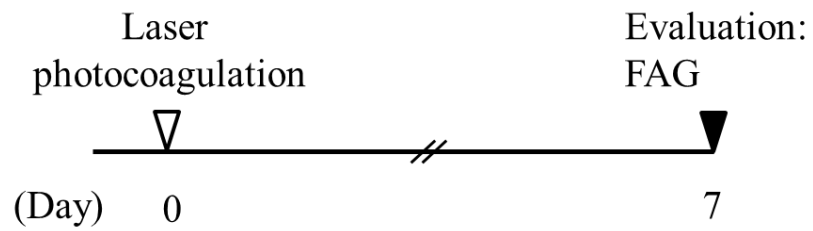

Figure 6 Timeline of study of laser-induced CNV in rats, including induction of impairment and evaluation

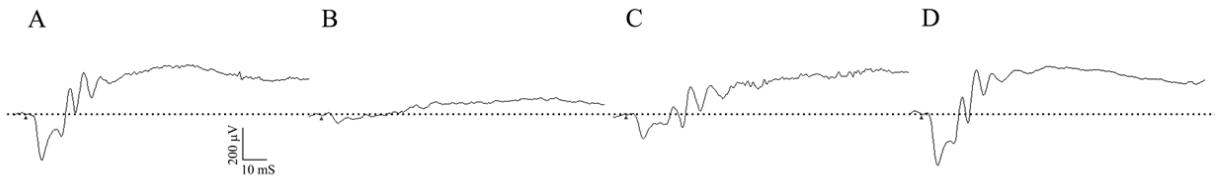

Figure 7 Representative ERG waveforms obtained 24 h after the light exposure

Trace from vehicle-treated mice without light exposure (A) Trace from vehicle-treated mice with light exposure (B) Trace from pramipexole (0.1 mg/kg body weight)-treated mice with light exposure (C) Trace from pramipexole (1 mg/kg body weight)-treated mice with light exposure (D) Pramipexole or vehicle was orally administered 1 h before light exposure.

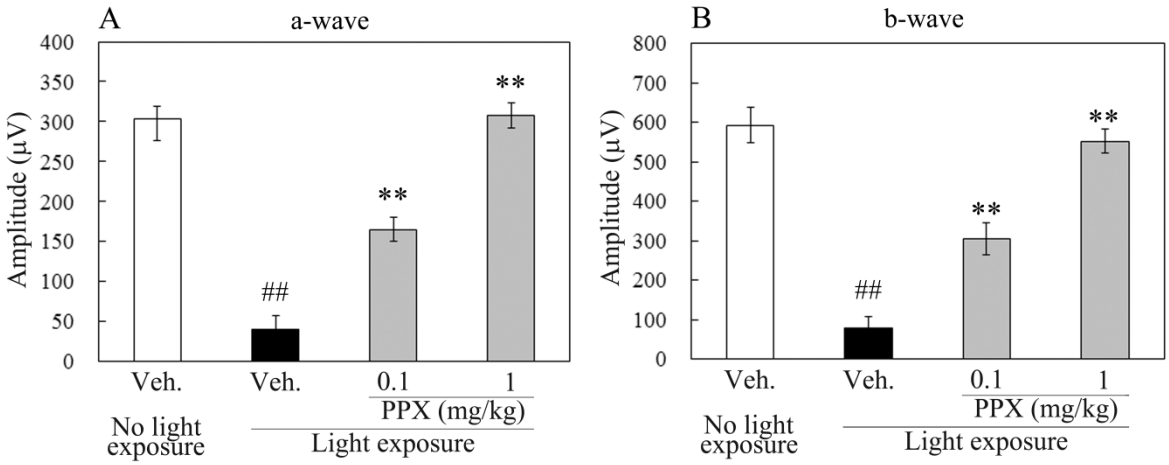

Figure 8 Effect of pramipexole on light-induced retinal dysfunction in mice in a- and b-waves of ERG

Pramipexole or vehicle was orally administered 1 h before light exposure. ERG was measured at 24 h after light exposure. Amplitudes of a- and b-wave (A and B). The data are shown as the mean ± SEM; n = 6 or 8. ##, $P < 0.01$ vs. vehicle-treated mice without light exposure. **, $P < 0.01$ vs. vehicle-treated mice with light exposure. Veh., Vehicle; PPX, Pramipexole.

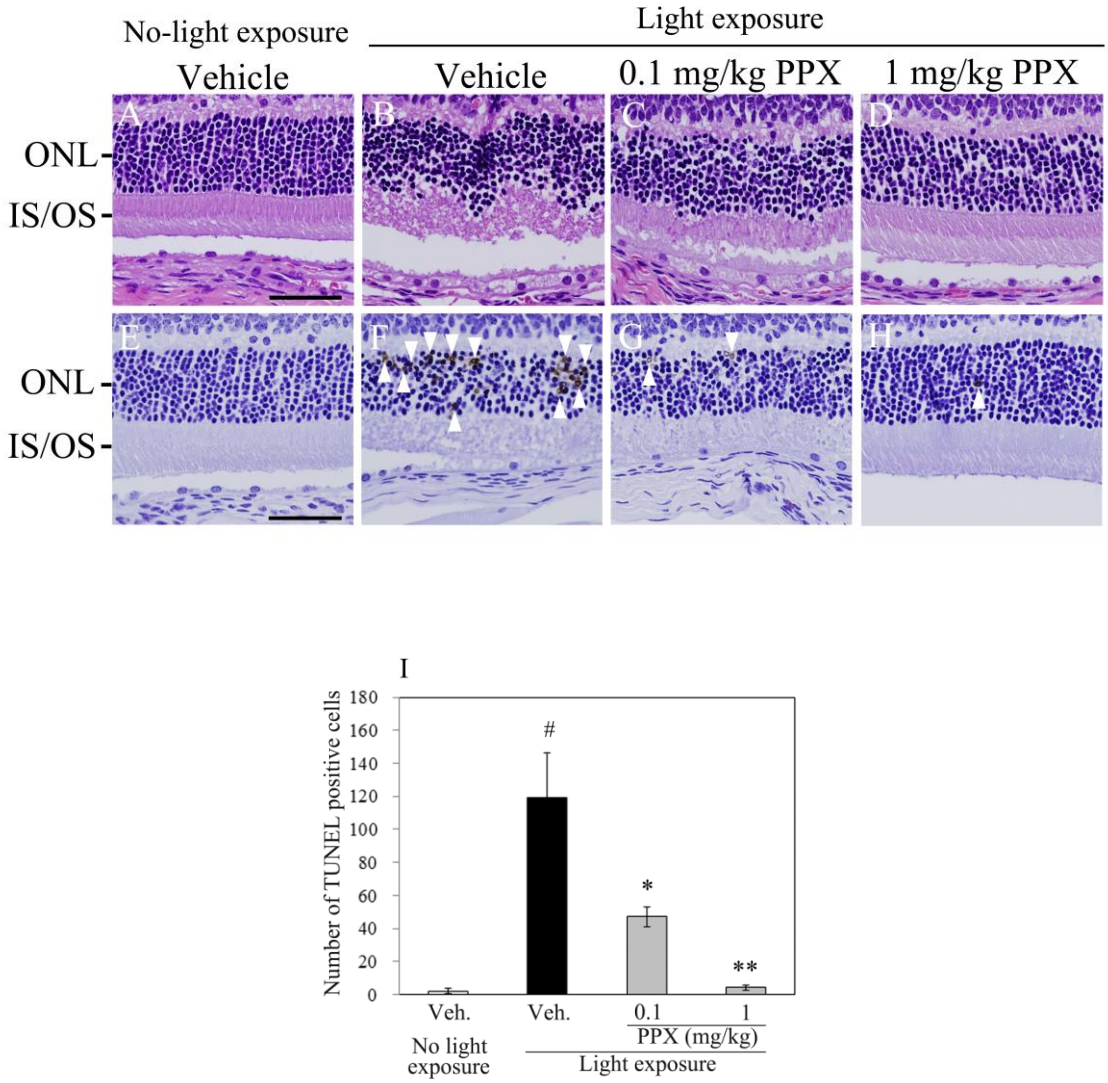

Figure 9 Effect of pramipexole on light-induced retinal damage in mice

Pramipexole was orally administered 1 h prior to light exposure. Eye samples were removed 24 h after light exposure for histopathological analysis (H&E staining; A-D, TUNEL staining; E-H). Vehicle treatment without light exposure (A and E). Vehicle treatment with light exposure (B and F). Pramipexole treatment at 0.1 mg/kg (C and G) or 1 mg/kg (D and H) doses with light exposure. Scale bar, 50 μm. White triangles indicate the TUNEL-positive cells. Quantitative analysis of the number of TUNEL-positive cells in the ONL (I). The data are shown as the mean ± SEM; n = 4. #, $P < 0.05$ vs. vehicle-treated mice without light exposure. *, $P < 0.05$; **, $P < 0.01$ vs. vehicle-treated mice with light exposure. Veh., Vehicle; PPX, Pramipexole.

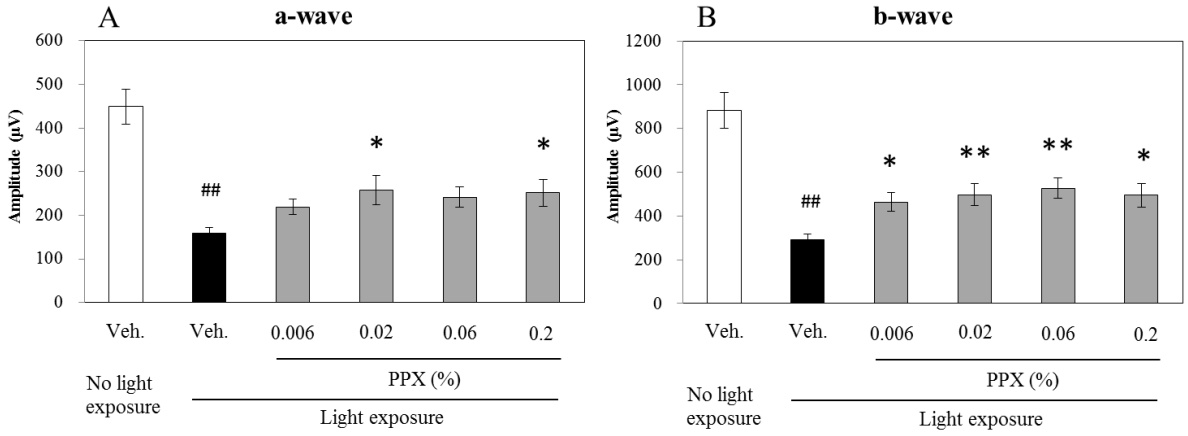

Figure 10 Effect of ocular instillation of pramipexole on light-induced retinal dysfunction in mice

Ocular instillation of pramipexole or vehicle was applied to cornea of mice 5 times a day every 1.5 h on the day before and the day of light exposure. ERG was measured at 24 h after light exposure. Amplitudes of a- and b-wave (A and B). The data are shown as the mean ± SEM; n = 8. ##, $P < 0.01$ vs. vehicle-treated mice without light exposure. *, $P < 0.05$, **, $P < 0.01$ vs. vehicle-treated mice with light exposure. Veh., Vehicle; PPX, Pramipexole.

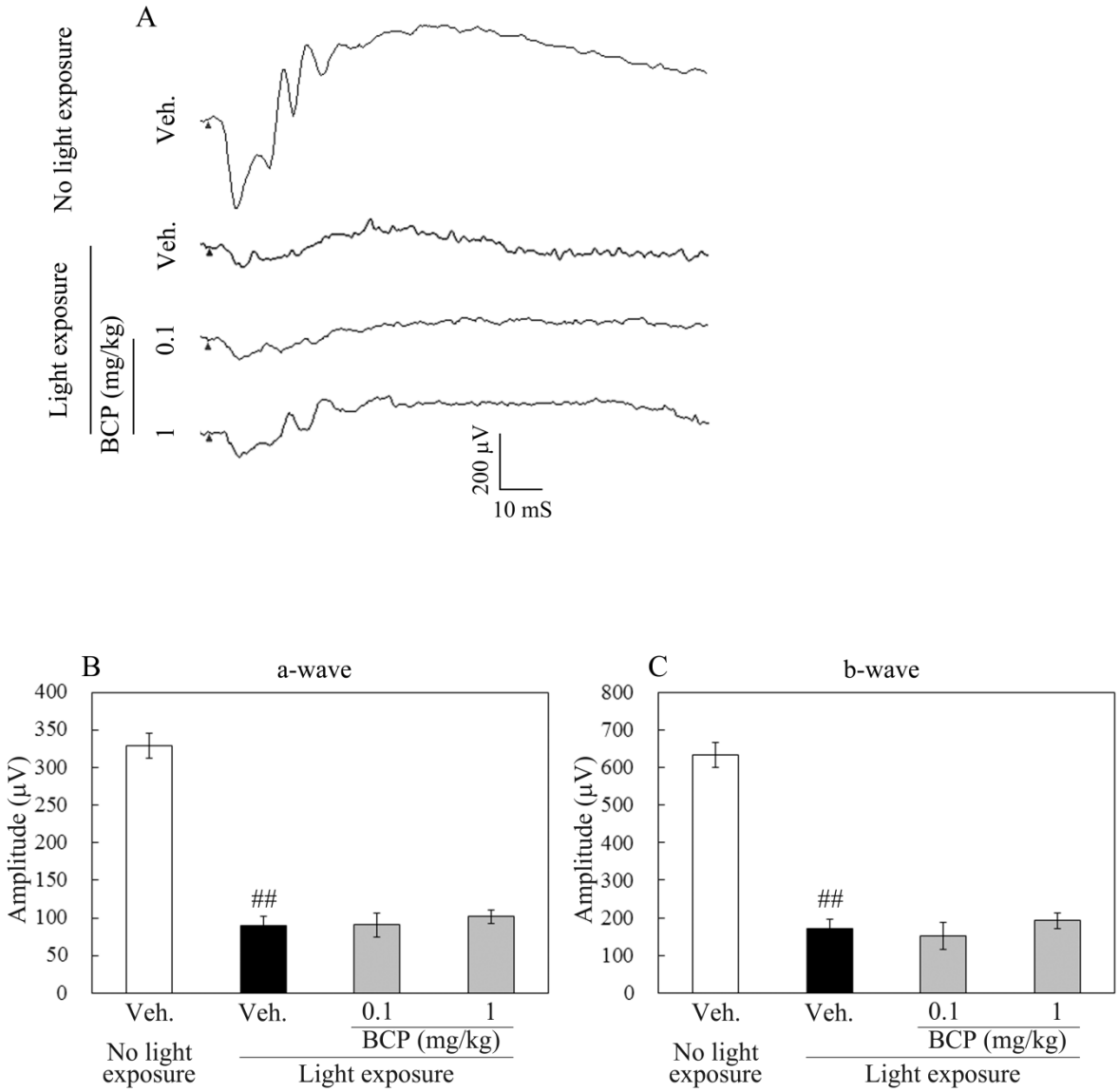

Figure 11 Effect of bromocriptine on light-induced retinal dysfunction in mice

Bromocriptine was orally administered 1 h before the light exposure. ERG was measured at 24 h after light exposure. Representative ERG wave responses (A). Amplitudes of the a- and b-waves (B and C). The data are shown as the mean ± SEM; n = 8. ##, $P < 0.01$ vs. vehicle-treated mice without light exposure. Veh., Vehicle; BCP, Bromocriptine.

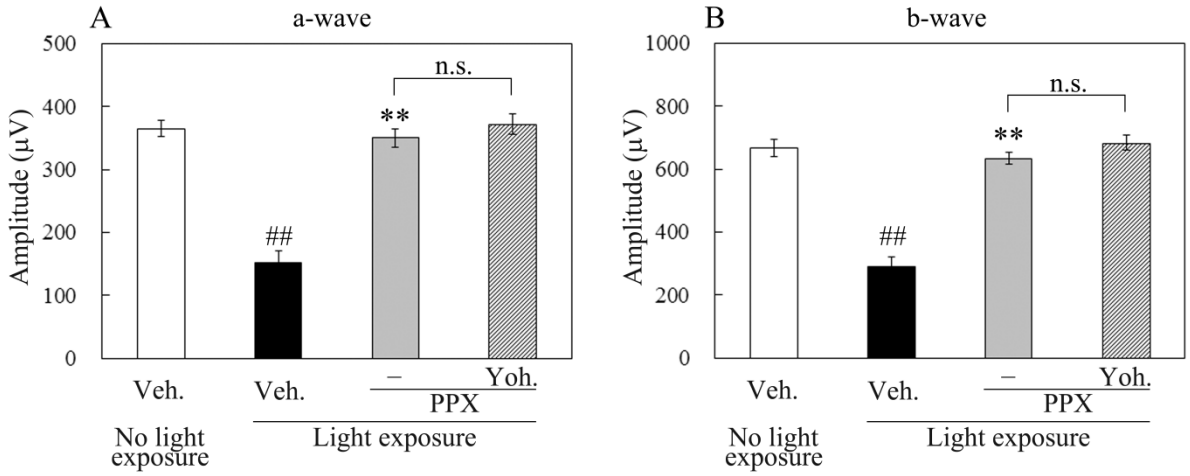

Figure 12 Influence of yohimbine, an alpha-2 adrenoceptor antagonist, on the protective effect of pramipexole against the light-induced retinal dysfunction in mice

Yohimbine (10 mg/kg body weight) was intraperitoneally injected 0.5 h prior to oral administration of pramipexole (1 mg/kg body weight). Mice were exposed to light 1 h after pramipexole administration. ERG was measured 24 h after the light exposure. Amplitudes of a- and b-waves (A and B). The data are shown as the mean ± SEM; n = 8. ##, $P < 0.01$ vs. vehicle-treated mice without light exposure. **, $P < 0.01$ vs. vehicle-treated mice with light exposure. Veh., Vehicle; PPX, Pramipexole; Yoh., Yohimbine; n.s., not significant.

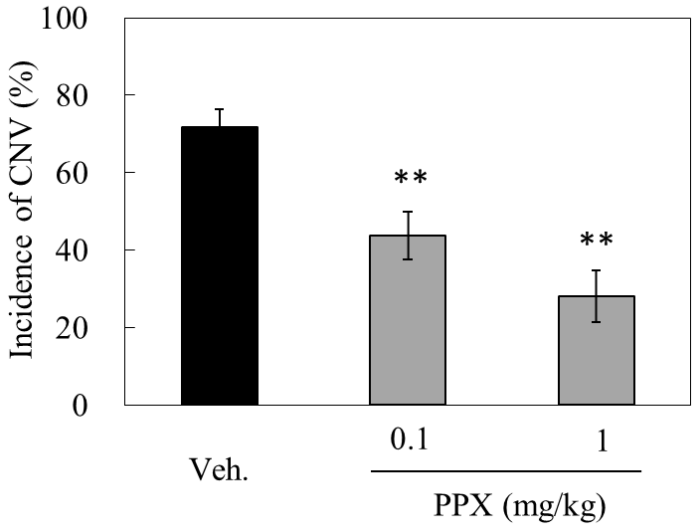

Figure 13 Effect of pramipexole on laser-induced CNV in rats

Pramipexole or vehicle was orally administered once a day for 7 days. On the day of laser photocoagulation, test articles were administrated just before the laser treatment, and then the administration was continued until 7 days after the laser treatment. CNV was observed by using fluorescein angiography at 7 days after the laser photocoagulation. The efficacy was evaluated by the incidence of CNV. The data are shown as the mean ± SEM; n = 8. **, $P <$ 0.01 vs. vehicle-treated rats with laser photocoagulation. Veh., Vehicle; PPX, Pramipexole.

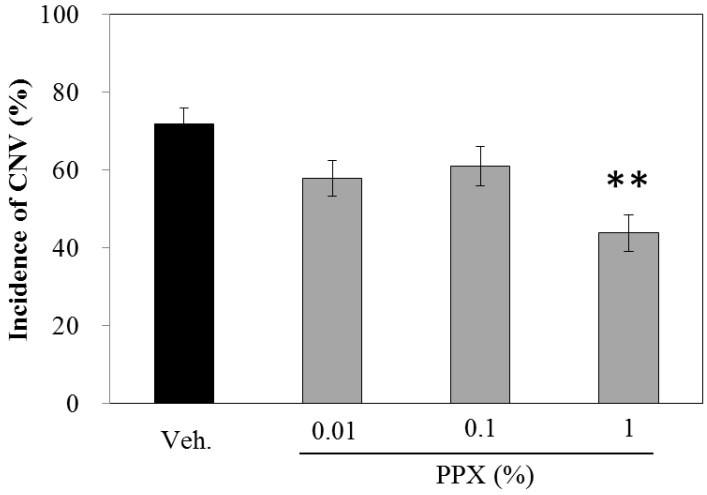

Figure 14 Effect of ocular instillation of pramipexole on laser-induced CNV in rats

Pramipexole solution was applied to cornea 6 times a day every 1.5 h. The instillation was started on the day of laser treatment, and continued for 7 days. CNV was observed by using fluorescein angiography at 7 days after the laser photocoagulation. The efficacy was evaluated by the incidence of CNV. The data are shown as the mean ± SEM; n = 8. **, $P < 0.01$ vs. vehicle-treated rats with laser photocoagulation. Veh., Vehicle; PPX, Pramipexole.

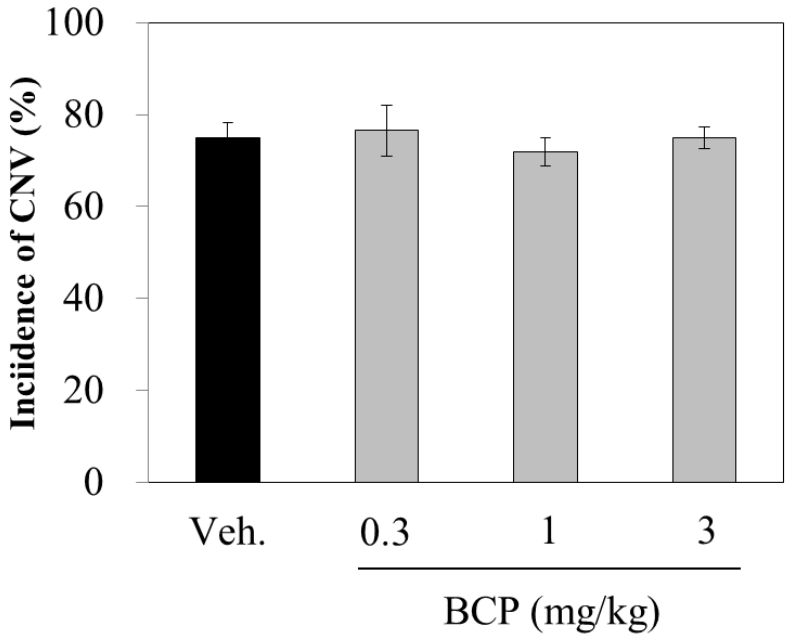

Figure 15 Effect of bromocriptine on laser-induced CNV in rats

Bromocriptine or vehicle was orally administered once a day for 7 days. On the day of laser photocoagulation, test articles were administrated just before the laser treatment, and then the administration was continued until 7 days after the laser treatment. CNV was observed by using fluorescein angiography at 7 days after the laser photocoagulation. The efficacy was evaluated by the incidence of CNV. The data are shown as the mean ± SEM; n = 8.Veh., Vehicle; BCP, Bromocriptine.

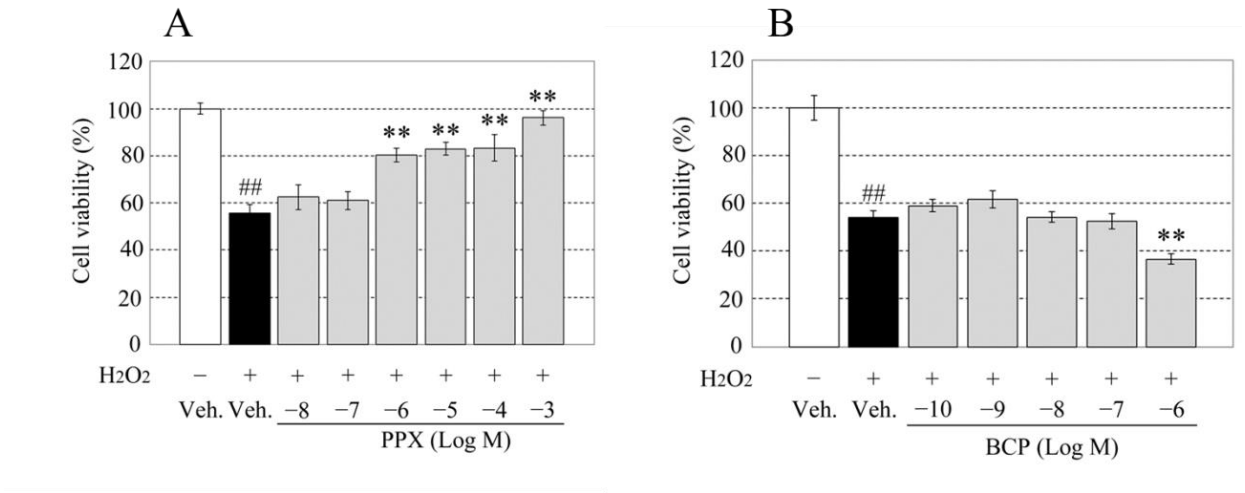

Figure 16 Effect of pramipexole and bromocriptine on H_2O_2-induced ARPE-19 cell death

ARPE-19 cells were pretreated with pramipexole (A) or bromocriptine (B) for 24 h prior to H_2O_2 treatment. Cell viability was measured by WST-8 assays. The data represent the percentage changes relative to the value of the untreated cell group. The data are shown as the mean ± SEM; n = 4. ##, $P < 0.01$ vs. untreated cells. **, $P < 0.01$ vs. H_2O_2 treated cells without experimental compound. Veh., Vehicle; PPX, Pramipexole; BCP, Bromocriptine

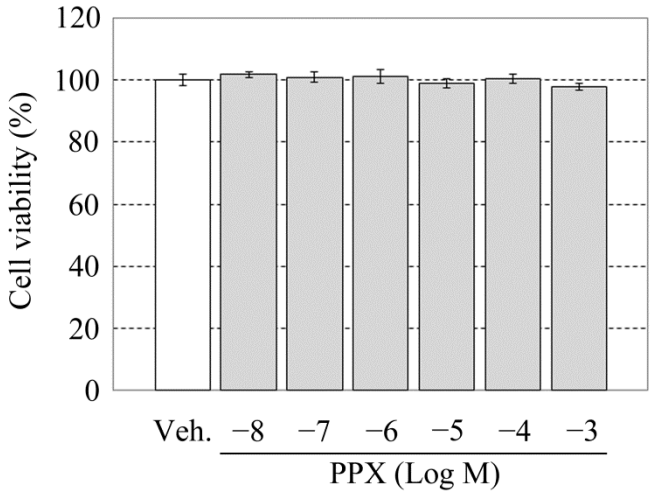

Figure 17 Effect of pramipexole on ARPE-19 cells proliferation

ARPE-19 cells were treated with pramipexole for 27 h. Cell viability was measured by WST-8 assays. The data represent the percent changes relative to the value of untreated cells. The data are shown as the mean ± SEM; n = 4. Veh., Vehicle; PPX, Pramipexole.

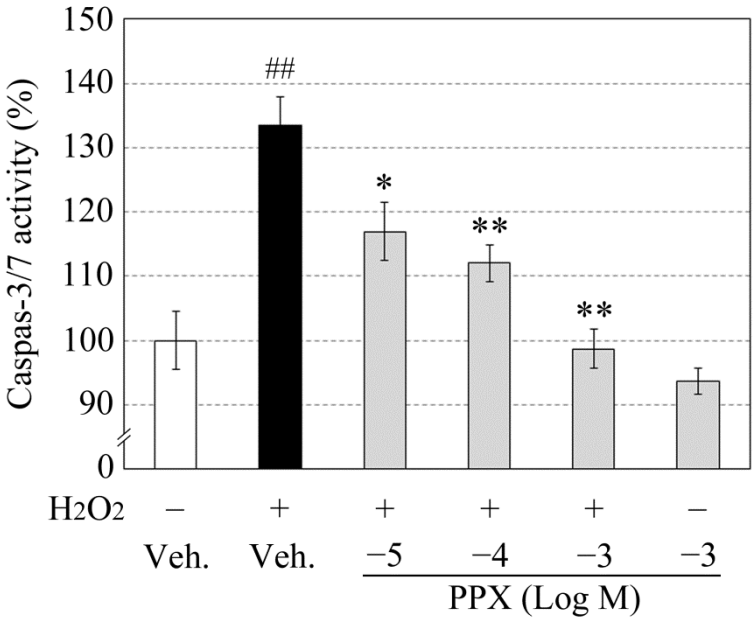

Figure 18 Effect of pramipexole on H_2O_2-induced caspase-3/7 activation in ARPE-19 cells

ARPE-19 cells were pretreated with pramipexole for 24 h prior to H_2O_2 treatment. Caspase-3/7 activity was measured using the Caspase-Glo 3/7 Assay kit. The data represent the percent changes relative to the values of the untreated cell group. The data are shown as the mean ± SEM; n = 6. ##, $P < 0.01$ vs. untreated cells. *, $P < 0.05$; **, $P < 0.01$ vs. H_2O_2-treated cells without the experimental compound. Veh., Vehicle; PPX, Pramipexole.

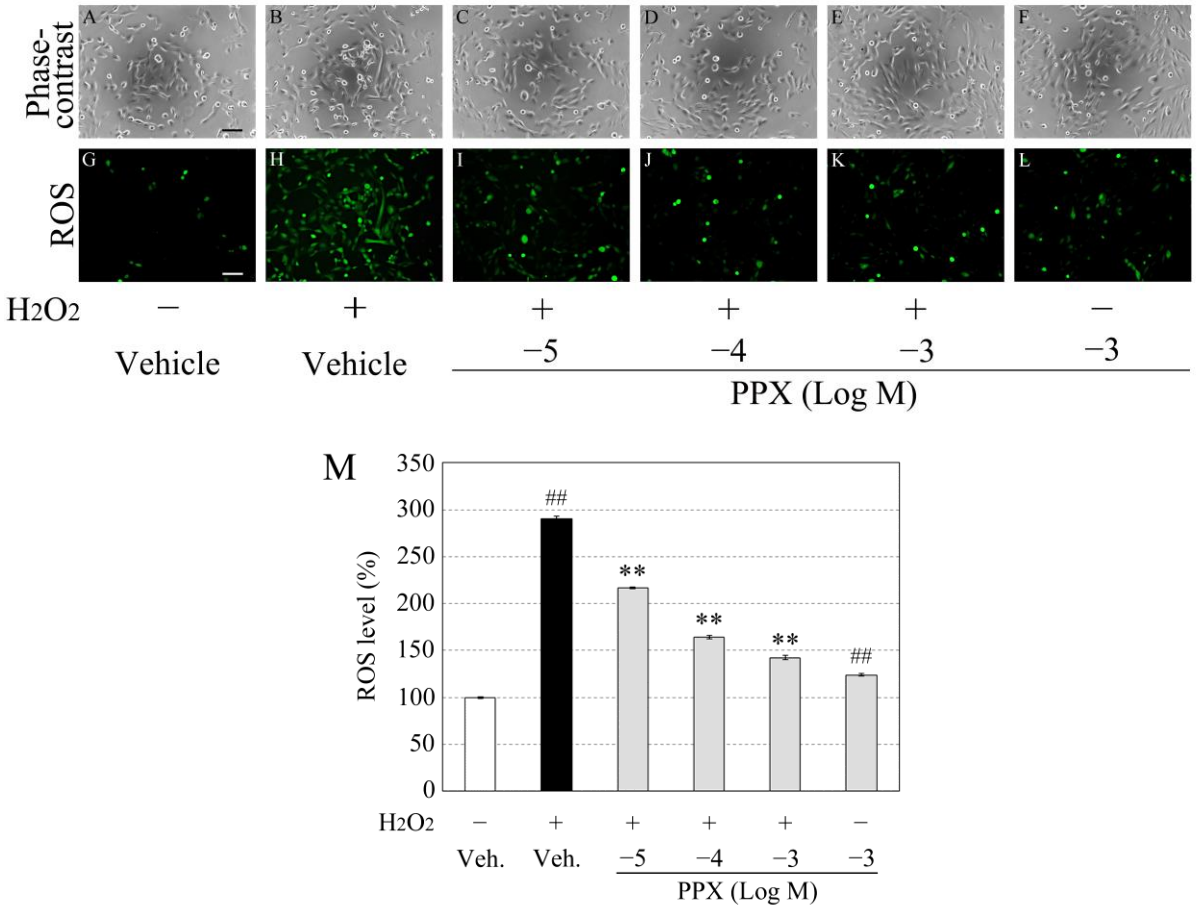

Figure 19 Effect of pramipexole on H_2O_2-induced intracellular ROS accumulation of ARPE-19 cells

ARPE-19 cells were pretreated with pramipexole for 24 h prior to H_2O_2 treatment. Intracellular ROS was detected using the OxiSelect intracellular ROS assay kit. Vehicle treatment without H_2O_2 (A and G). Vehicle treatment with H_2O_2 (B and H). Pramipexole treatment at concentrations of 10^{-5} M (C and I), 10^{-4} M (D and J), or 10^{-3} M (E and K) with H_2O_2. Pramipexole alone treatment at 10^{-3} M (F and L). Scale bar, 100 μm. Quantitative analysis of the ROS accumulation in cells (M). The data represent the percent changes relative to the values of untreated cell group. The data are shown as the mean ± SEM; n = 6. ##, $P < 0.01$ vs. untreated cells. **, $P < 0.01$ vs. H_2O_2-treated cells without the experimental compound. Veh., Vehicle; PPX, Pramipexole.

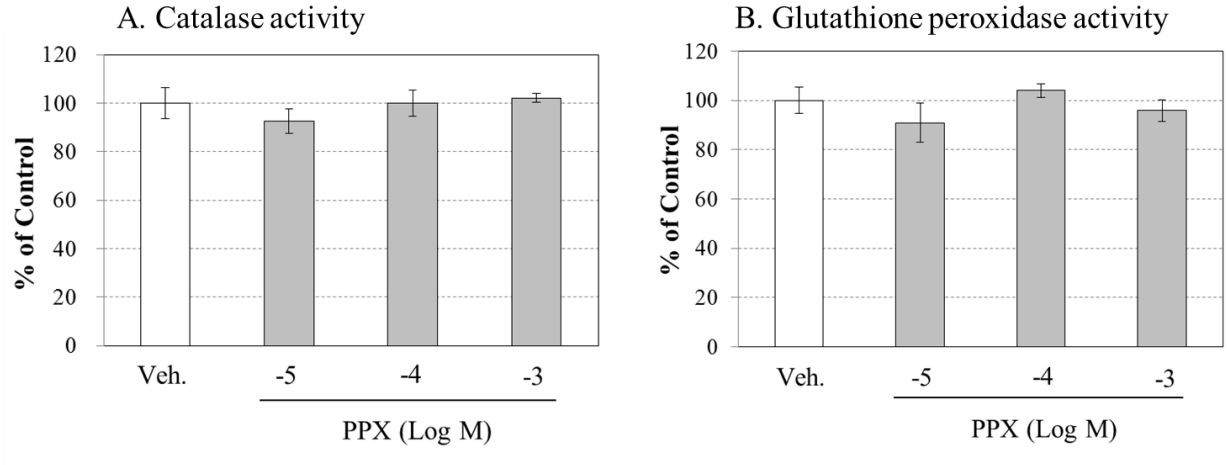

Figure 20 Effect of pramipexole on catalase and glutathione peroxidase activity in ARPE-19 cells

ARPE-19 cells were pretreated with pramipexole for 27 h. Catalase activity (A) and glutathione peroxidase (B) of cell lysate were measured by catalase assay kit and glutathione peroxidase assay kit, respectively. The data represent the percent changes relative to the value of untreated cell group. The data are shown as the mean ± SEM; n = 4. Veh., Vehicle; PPX, Pramipexole.

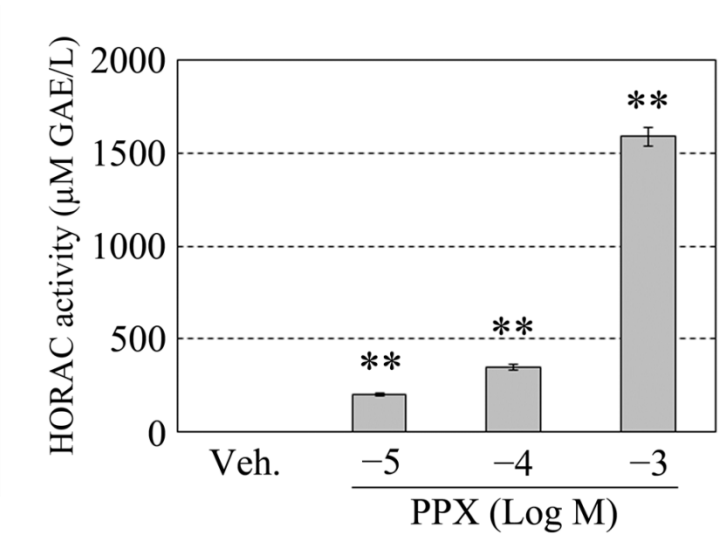

Figure 21 Hydroxyl radical scavenging activity of pramipexole

The hydroxyl radical scavenging activity of pramipexole was measured using a HORAC Activity Assay kit. The antioxidant activity of pramipexole was calculated relative to the concentration of gallic acid, which is the antioxidant standard in this assay. The data are shown as the mean ± SEM of four independent experiments. **, $P < 0.01$ vs.Vehicle. Veh., Vehicle; PPX, Pramipexole.

7. REFERENCES

1. Resnikoff S, Pascolini D, Etya'ale D, et al. Global data on visual impairment in the year 2002. *Bull World Health Organ* 2004;82:844-851.

2. Kaarniranta K, Salminen A. Age-related macular degeneration: activation of innate immunity system via pattern recognition receptors. *J Mol Med (Berl)* 2009;87:117-123.

3. Marsiglia M, Boddu S, Bearelly S, et al. Association between geographic atrophy progression and reticular pseudodrusen in eyes with dry age-related macular degeneration. *Invest Ophthalmol Vis Sci* 2013;54:7362-7369.

4. Bowes Rickman C, Farsiu S, Toth CA, Klingeborn M. Dry age-related macular degeneration: mechanisms, therapeutic targets, and imaging. *Invest Ophthalmol Vis Sci* 2013;54:ORSF68-80.

5. Bird AC, Phillips RL, Hageman GS. Geographic atrophy: a histopathological assessment. *JAMA ophthalmology* 2014;132:338-345.

6. Hartnett ME, Elsner AE. Characteristics of exudative age-related macular degeneration determined in vivo with confocal and indirect infrared imaging. *Ophthalmology* 1996;103:58-71.

7. Kovach JL, Schwartz SG, Flynn HW, Jr., Scott IU. Anti-VEGF Treatment Strategies for Wet AMD. *J Ophthalmol* 2012;2012:786870.

8. Rosenfeld PJ, Brown DM, Heier JS, et al. Ranibizumab for neovascular age-related macular degeneration. *N Engl J Med* 2006;355:1419-1431.

9. Yu Y, Reynolds R, Rosner B, Daly MJ, Seddon JM. Prospective assessment of genetic effects on progression to different stages of age-related macular degeneration using multistate Markov models. *Invest Ophthalmol Vis Sci* 2012;53:1548-1556.

10. Seddon JM, Reynolds R, Yu Y, Daly MJ, Rosner B. Risk models for progression to advanced age-related macular degeneration using demographic, environmental, genetic, and ocular factors. *Ophthalmology* 2011;118:2203-2211.

11. Delcourt C, Diaz JL, Ponton-Sanchez A, Papoz L. Smoking and age-related macular degeneration. The POLA Study. Pathologies Oculaires Liees a l'Age. *Arch Ophthalmol* 1998;116:1031-1035.

12. Klein RJ, Zeiss C, Chew EY, et al. Complement factor H polymorphism in age-related macular degeneration. *Science* 2005;308:385-389.

13. Haines JL, Hauser MA, Schmidt S, et al. Complement factor H variant increases the risk of age-related macular degeneration. *Science* 2005;308:419-421.

14. Edwards AO, Ritter R, 3rd, Abel KJ, Manning A, Panhuysen C, Farrer LA. Complement factor H polymorphism and age-related macular degeneration. *Science* 2005;308:421-424.

15. Gold B, Merriam JE, Zernant J, et al. Variation in factor B (BF) and complement component 2 (C2) genes is associated with age-related macular degeneration. *Nat Genet* 2006;38:458-462.

16. Yates JR, Sepp T, Matharu BK, et al. Complement C3 variant and the risk of age-related macular degeneration. *N Engl J Med* 2007;357:553-561.

17. Mullins RF, Russell SR, Anderson DH, Hageman GS. Drusen associated with aging and age-related macular degeneration contain proteins common to extracellular deposits associated with atherosclerosis, elastosis, amyloidosis, and dense deposit disease. *FASEB J* 2000;14:835-846.

18. Masutomi K, Chen C, Nakatani K, Koutalos Y. All-trans retinal mediates light-induced oxidation in single living rod photoreceptors. *Photochem Photobiol* 2012;88:1356-1361.

19. Eldred GE, Lasky MR. Retinal age pigments generated by self-assembling lysosomotropic detergents. *Nature* 1993;361:724-726.

20. Holz FG, Bellmann C, Margaritidis M, Schutt F, Otto TP, Volcker HE. Patterns of increased in vivo fundus autofluorescence in the junctional zone of geographic atrophy of the retinal pigment epithelium associated with age-related macular degeneration. *Graefes Arch Clin Exp Ophthalmol* 1999;237:145-152.

21. Dorey CK, Wu G, Ebenstein D, Garsd A, Weiter JJ. Cell loss in the aging retina. Relationship to lipofuscin accumulation and macular degeneration. *Invest Ophthalmol Vis Sci* 1989;30:1691-1699.

22. Rozanowska M, Jarvis-Evans J, Korytowski W, Boulton ME, Burke JM, Sarna T. Blue light-induced reactivity of retinal age pigment. In vitro generation of oxygen-reactive species. *J Biol Chem* 1995;270:18825-18830.

23. Hahn P, Milam AH, Dunaief JL. Maculas affected by age-related macular degeneration contain increased chelatable iron in the retinal pigment epithelium and Bruch's membrane. *Arch Ophthalmol* 2003;121:1099-1105.

24. Shen JK, Dong A, Hackett SF, Bell WR, Green WR, Campochiaro PA. Oxidative damage in age-related macular degeneration. *Histol Histopathol* 2007;22:1301-1308.

25. Zhang J, Perry G, Smith MA, et al. Parkinson's disease is associated with oxidative damage to cytoplasmic DNA and RNA in substantia nigra neurons. *Am J Pathol* 1999;154:1423-1429.

26. Halliwell B. Reactive oxygen species and the central nervous system. *J Neurochem* 1992;59:1609-1623.

27. Zuo L, Motherwell MS. The impact of reactive oxygen species and genetic mitochondrial mutations in Parkinson's disease. *Gene* 2013;532:18-23.

28. Adam-Vizi V. Production of reactive oxygen species in brain mitochondria: contribution by electron transport chain and non-electron transport chain sources. *Antioxidants & redox signaling* 2005;7:1140-1149.

29. Dexter DT, Wells FR, Lees AJ, et al. Increased nigral iron content and alterations in other metal ions occurring in brain in Parkinson's disease. *J Neurochem* 1989;52:1830-1836.

30. Yoritaka A, Hattori N, Uchida K, Tanaka M, Stadtman ER, Mizuno Y. Immunohistochemical detection of 4-hydroxynonenal protein adducts in Parkinson disease. *Proc Natl Acad Sci U S A* 1996;93:2696-2701.

31. Clarke CE, Guttman M. Dopamine agonist monotherapy in Parkinson's disease. *Lancet* 2002;360:1767-1769.

32. Newman-Tancredi A, Cussac D, Audinot V, et al. Differential actions of antiparkinson agents at multiple classes of monoaminergic receptor. II. Agonist and antagonist properties at subtypes of dopamine D(2)-like receptor and alpha(1)/alpha(2)-adrenoceptor. *J Pharmacol Exp Ther* 2002;303:805-814.

33. Yukoyama K, Oiwa Y, Imanishi R, et al. Studies on the Metabolic Fate of Pramipexole (SND 919 CL2Y) (I): Absorption, Distribution and Excretion after a Single Oral Administration to Rats. *Yakubutsu Dotai* 1999;14:9.

34. Benbir G, Guilleminault C. Pramipexole: new use for an old drug - the potential use of pramipexole in the treatment of restless legs syndrome. *Neuropsychiatr Dis Treat* 2006;2:393-405.

35. Kitamura Y, Kosaka T, Kakimura JI, et al. Protective effects of the antiparkinsonian drugs talipexole and pramipexole against 1-methyl-4-phenylpyridinium-induced apoptotic death in human neuroblastoma SH-SY5Y cells. *Mol Pharmacol* 1998;54:1046-1054.

36. Fujita Y, Izawa Y, Ali N, et al. Pramipexole protects against H2O2-induced PC12 cell death. *Naunyn Schmiedebergs Arch Pharmacol* 2006;372:257-266.

37. Inden M, Kitamura Y, Tamaki A, et al. Neuroprotective effect of the antiparkinsonian drug pramipexole against nigrostriatal dopaminergic degeneration in rotenone-treated mice. *Neurochem Int* 2009;55:760-767.

38. Cassarino DS, Fall CP, Smith TS, Bennett JP, Jr. Pramipexole reduces reactive oxygen species production in vivo and in vitro and inhibits the mitochondrial permeability transition produced by the parkinsonian neurotoxin methylpyridinium ion. *J Neurochem* 1998;71:295-301.

39. Zou L, Xu J, Jankovic J, He Y, Appel SH, Le W. Pramipexole inhibits lipid peroxidation and reduces injury in the substantia nigra induced by the dopaminergic neurotoxin 1-methyl-4-phenyl-1,2,3,6-tetrahydropyridine in C57BL/6 mice. *Neurosci Lett* 2000;281:167-170.

40. Lafuente MP, Villegas-Perez MP, Sobrado-Calvo P, Garcia-Aviles A, Miralles de Imperial J, Vidal-Sanz M. Neuroprotective effects of alpha(2)-selective adrenergic agonists against ischemia-induced retinal ganglion cell death. *Invest Ophthalmol Vis Sci* 2001;42:2074-2084.

41. Tanito M, Yoshida Y, Kaidzu S, Ohira A, Niki E. Detection of lipid peroxidation in light-exposed mouse retina assessed by oxidative stress markers, total hydroxyoctadecadienoic acid and 8-iso-prostaglandin F2alpha. *Neurosci Lett* 2006;398:63-68.

42. Yoneda S, Tanaka E, Goto W, Ota T, Hara H. Topiramate reduces excitotoxic and ischemic injury in the rat retina. *Brain Res* 2003;967:257-266.

43. Shimazaki H, Hironaka K, Fujisawa T, et al. Edaravone-loaded liposome eyedrops protect against light-induced retinal damage in mice. *Invest Ophthalmol Vis Sci* 2011;52:7289-7297.

44. Imai S, Shimazawa M, Nakanishi T, Tsuruma K, Hara H. Calpain inhibitor protects cells against light-induced retinal degeneration. *J Pharmacol Exp Ther* 2010;335:645-652.

45. Imai S, Inokuchi Y, Nakamura S, Tsuruma K, Shimazawa M, Hara H. Systemic administration of a free radical scavenger, edaravone, protects against light-induced photoreceptor degeneration in the mouse retina. *Eur J Pharmacol* 2010;642:77-85.

46. Doukas J, Mahesh S, Umeda N, et al. Topical administration of a multi-targeted kinase inhibitor suppresses choroidal neovascularization and retinal edema. *J Cell Physiol* 2008;216:29-37.

47. Yafai Y, Yang XM, Niemeyer M, et al. Anti-angiogenic effects of the receptor tyrosine kinase inhibitor, pazopanib, on choroidal neovascularization in rats. *Eur J Pharmacol* 2011;666:12-18.

48. Tsuruma K, Tanaka Y, Shimazawa M, Mashima Y, Hara H. Unoprostone reduces oxidative stress- and light-induced retinal cell death, and phagocytotic dysfunction, by activating BK channels. *Mol Vis* 2011;17:3556-3565.

49. Spencer ML, Shao H, Andres DA. Induction of neurite extension and survival in pheochromocytoma cells by the Rit GTPase. *J Biol Chem* 2002;277:20160-20168.

50. Roth C, Pantel K, Muller V, et al. Apoptosis-related deregulation of proteolytic activities and high serum levels of circulating nucleosomes and DNA in blood correlate with breast cancer progression. *BMC cancer* 2011;11:4.

51. Song H, Wohltmann M, Tan M, Ladenson JH, Turk J. Group VIA phospholipase A2 mitigates palmitate-induced beta-cell mitochondrial injury and apoptosis. *J Biol Chem* 2014;289:14194-14210.

52. Jeong MH, Yang KM, Jeong DH, et al. Protective activity of a novel resveratrol analogue, HS-1793, against DNA damage in 137Cs-irradiated CHO-K1 cells. *J Radiat Res* 2014;55:464-475.

53. Jiang CP, Ding H, Shi DH, Wang YR, Li EG, Wu JH. Pro-apoptotic effects of tectorigenin on human hepatocellular carcinoma HepG2 cells. *World journal of gastroenterology : WJG* 2012;18:1753-1764.

54. Kakimura J, Kitamura Y, Takata K, Kohno Y, Nomura Y, Taniguchi T. Release and aggregation of cytochrome c and alpha-synuclein are inhibited by the antiparkinsonian drugs, talipexole and pramipexole. *Eur J Pharmacol* 2001;417:59-67.

55. Li C, Guo Y, Xie W, Li X, Janokovic J, Le W. Neuroprotection of pramipexole in UPS impairment induced animal model of Parkinson's disease. *Neurochem Res* 2010;35:1546-1556.

56. Carvey PM, Pieri S, Ling ZD. Attenuation of levodopa-induced toxicity in mesencephalic cultures by pramipexole. *J Neural Transm* 1997;104:209-228.

57. Ramirez AD, Wong SK, Menniti FS. Pramipexole inhibits MPTP toxicity in mice by dopamine D3 receptor dependent and independent mechanisms. *Eur J Pharmacol* 2003;475:29-35.

58. Tanito M, Nishiyama A, Tanaka T, et al. Change of redox status and modulation by thiol replenishment in retinal photooxidative damage. *Invest Ophthalmol Vis Sci* 2002;43:2392-2400.

59. Tomita H, Kotake Y, Anderson RE. Mechanism of protection from light-induced retinal degeneration by the synthetic antioxidant phenyl-N-tert-butylnitrone. *Invest Ophthalmol Vis Sci* 2005;46:427-434.

60. Cruickshanks KJ, Klein R, Klein BE. Sunlight and age-related macular degeneration. The Beaver Dam Eye Study. *Arch Ophthalmol* 1993;111:514-518.

61. Dunaief JL, Dentchev T, Ying GS, Milam AH. The role of apoptosis in age-related macular degeneration. *Arch Ophthalmol* 2002;120:1435-1442.

62. Hall ED, Andrus PK, Oostveen JA, Althaus JS, VonVoigtlander PF. Neuroprotective effects of the dopamine D2/D3 agonist pramipexole against postischemic or methamphetamine-induced degeneration of nigrostriatal neurons. *Brain Res* 1996;742:80-88.

63. Kvernmo T, Hartter S, Burger E. A review of the receptor-binding and pharmacokinetic properties of dopamine agonists. *Clin Ther* 2006;28:1065-1078.

64. Lane EL, Dunnett SB. Pre-treatment with dopamine agonists influence L-dopa mediated rotations without affecting abnormal involuntary movements in the 6-OHDA lesioned rat. *Behav Brain Res* 2010;213:66-72.

65. Derouiche A, Asan E. The dopamine D2 receptor subfamily in rat retina: ultrastructural immunogold and in situ hybridization studies. *Eur J Neurosci* 1999;11:1391-1402.

66. Lee D, Kim KY, Noh YH, et al. Brimonidine blocks glutamate excitotoxicity-induced oxidative stress and preserves mitochondrial transcription factor a in ischemic retinal injury. *PloS one* 2012;7:e47098.

67. Lee J, Park DY, Park do Y, et al. Angiopoietin-1 suppresses choroidal neovascularization and vascular leakage. *Invest Ophthalmol Vis Sci* 2014;55:2191-2199.

68. Hara C, Kasai A, Gomi F, et al. Laser-induced choroidal neovascularization in mice attenuated by deficiency in the apelin-APJ system. *Invest Ophthalmol Vis Sci* 2013;54:4321-4329.

69. Monaghan-Benson E, Hartmann J, Vendrov AE, et al. The role of vascular endothelial growth factor-induced activation of NADPH oxidase in choroidal endothelial cells and choroidal neovascularization. *Am J Pathol* 2010;177:2091-2102.

70. Yamashita H, Horie K, Yamamoto T, Nagano T, Hirano T. Light-induced retinal damage in mice. Hydrogen peroxide production and superoxide dismutase activity in retina. *Retina* 1992;12:59-66.

71. Tanito M, Elliott MH, Kotake Y, Anderson RE. Protein modifications by 4-hydroxynonenal and 4-hydroxyhexenal in light-exposed rat retina. *Invest Ophthalmol Vis Sci* 2005;46:3859-3868.

72. Hara R, Inomata Y, Kawaji T, et al. Suppression of choroidal neovascularization by N-acetyl-cysteine in mice. *Curr Eye Res* 2010;35:1012-1020.

73. Venza I, Visalli M, Cucinotta M, Teti D, Venza M. Association between oxidative stress and macromolecular damage in elderly patients with age-related macular degeneration. *Aging Clin Exp Res* 2012;24:21-27.

74. Jia L, Dong Y, Yang H, Pan X, Fan R, Zhai L. Serum superoxide dismutase and malondialdehyde levels in a group of Chinese patients with age-related macular degeneration. *Aging Clin Exp Res* 2011;23:264-267.

75. Li P, Nijhawan D, Budihardjo I, et al. Cytochrome c and dATP-dependent formation of Apaf-1/caspase-9 complex initiates an apoptotic protease cascade. *Cell* 1997;91:479-489.

76. Boatright KM, Salvesen GS. Mechanisms of caspase activation. *Curr Opin Cell Biol* 2003;15:725-731.

77. Inokuchi Y, Imai S, Nakajima Y, et al. Edaravone, a free radical scavenger, protects against retinal damage in vitro and in vivo. *J Pharmacol Exp Ther* 2009;329:687-698.

78. Age-Related Eye Disease Study Research Group. A randomized, placebo-controlled, clinical trial of high-dose supplementation with vitamins C and E, beta carotene, and zinc for age-related macular degeneration and vision loss: AREDS report no. 8. *Arch Ophthalmol* 2001;119:1417-1436.

79. Pattee GL, Post GR, Gerber RE, Bennett JP, Jr. Reduction of oxidative stress in amyotrophic lateral sclerosis following pramipexole treatment. *Amyotrophic lateral sclerosis and other motor neuron disorders : official publication of the World Federation of Neurology, Research Group on Motor Neuron Diseases* 2003;4:90-95.